Hamiltonicity for convex shape Delaunay and Gabriel graphs *

Prosenjit Bose[1], Pilar Cano[1,2], Maria Saumell[3,4], and Rodrigo I. Silveira[2]

[1] *School of Computer Science, Carleton University, Ottawa*
[2] *Departament de Matemàtiques, Universitat Politècnica de Catalunya*
[3] *The Czech Academy of Sciences, Institute of Computer Science*
[4] *Department of Theoretical Computer Science, Faculty of Information Technology, Czech Technical University in Prague*

March 4, 2020

Abstract

We study Hamiltonicity for some of the most general variants of Delaunay and Gabriel graphs. Instead of defining these proximity graphs using circles, we use an arbitrary convex shape $\mathcal{C}$. Let S be a point set in the plane. The k-order Delaunay graph of S, denoted k-$DG_{\mathcal{C}}(S)$, has vertex set S, and edges defined as follows. Given $p, q \in S$, pq is an edge of k-$DG_{\mathcal{C}}(S)$ provided there exists *some* homothet of $\mathcal{C}$ with p and q on its boundary and containing at most k points of S different from p and q. The k-order Gabriel graph, denoted k-$GG_{\mathcal{C}}(S)$, is defined analogously, except that the homothets considered are restricted to be *smallest* homothets of $\mathcal{C}$ with p and q on the boundary.

We provide upper bounds on the minimum value of k for which k-$GG_{\mathcal{C}}(S)$ is Hamiltonian. Since k-$GG_{\mathcal{C}}(S) \subseteq k$-$DG_{\mathcal{C}}(S)$, all results carry over to k-$DG_{\mathcal{C}}(S)$. In particular, we give upper bounds of 24 for every $\mathcal{C}$ and 15 for every point-symmetric $\mathcal{C}$. We also improve these bounds to 7 for squares, 11 for regular hexagons, 12 for regular octagons, and 11 for even-sided regular t-gons (for $t \geq 10$). These constitute the first general results on Hamiltonicity for convex shape Delaunay and Gabriel graphs.

In addition, we show lower bounds of $k = 3$ and $k = 6$ on the existence of a bottleneck Hamiltonian cycle in the k-order Gabriel graph for squares and hexagons, respectively. Finally, we construct a point set such that for an infinite family of regular polygons $\mathcal{P}_t$, the Delaunay graph $DG_{\mathcal{P}_t}$ does not contain a Hamiltonian cycle.

1 Introduction

The study of the combinatorial properties of geometric graphs has played an important role in the area of Discrete and Computational Geometry. One of the fundamental structures that has been studied intensely is the Delaunay triangulation of a planar point set and some of its spanning subgraphs, such as the Gabriel Graph, the Relative Neighborhood Graph and

*P.B. was partially supported by NSERC. P.C. was supported by CONACyT. M.S. was supported by the Czech Science Foundation, grant number GJ19-06792Y, and by institutional support RVO:67985807. R.S. was supported by MINECO through the Ramón y Cajal program. P.C. and R.S. were also supported by projects MINECO MTM2015-63791-R and Gen. Cat. 2017SGR1640. This project has received funding from the European Union's Horizon 2020 research and innovation programme under the Marie Skłodowska-Curie grant agreement No 734922.

the Minimum Spanning Tree. Delaunay triangulations possess many interesting properties. For example, among all triangulations of a given planar point set, the Delaunay triangulation maximizes the minimum angle. It is also a 1.99-spanner [20] (i.e., for any pair of vertices x, y, the shortest path between x and y in the Delaunay triangulation has length that is at most 1.99 times $|xy|$). See [17] for an encyclopedic treatment of this structure and its many properties.

Shamos [19] conjectured that the Delaunay triangulation contains a Hamiltonian cycle. This conjecture sparked a flurry of research activity. Although Dillencourt [11] disproved this conjecture, he showed that Delaunay triangulations are *almost* Hamiltonian [12], that is, they are 1-tough.[1] Focus then shifted on determining how much to loosen the definition of the Delaunay triangulation to achieve Hamiltonicity. One such direction is to relax the *empty disk* requirement. Given a planar point set S and two points $p, q \in S$, the k-Delaunay graph (k-DG) with vertex set S has an edge pq provided that there exists a closed disk with p and q on its boundary containing at most k points of S different from p and q.[2] If the disk with p and q on its boundary is restricted to disks with pq as diameter, then the graph is called the k-Gabriel graph (k-GG). For the k-Relative Neighborhood graph (k-RNG), pq is an edge provided that there are at most k points of S whose distance to both p and q is less than $|pq|$. Note that $k\text{-}RNG \subseteq k\text{-}GG \subseteq k\text{-}DG$. Chang et al. [9] showed that 19-RNG is Hamiltonian.[3] Abellanas et al. [1] proved that 15-GG is Hamiltonian. Currently, the lowest known upper bound is by Kaiser et al. [15] who showed that 10-GG is Hamiltonian. All of these results are obtained by studying properties of *bottleneck Hamiltonian cycles*. Given a planar point set, a bottleneck Hamiltonian cycle is a Hamiltonian cycle whose maximum edge length is minimum among all Hamiltonian cycles of the point set. Biniaz et al. [5] showed that there exist point sets such that its 7-GG does not contain a bottleneck Hamiltonian cycle, implying that this approach cannot yield an upper bound lower than 8. Despite this, it is conjectured that 1-DG is Hamiltonian [1].

Another avenue that has been explored is the relaxation of the shape defining the Delaunay triangulation. Delaunay graphs where the disks have been replaced by various convex shapes have been studied in the literature. For instance, Chew [10] showed that the $\triangle$-Delaunay graph (i.e., where the shape is an equilateral triangle instead of a disk), denoted $DG_\triangle$, is a 2-spanner and that the $\square$-Delaunay graph (i.e., where the disk is replaced by a square), denoted $DG_\square$, is a $\sqrt{10}$-spanner. Bose et al. [8] proved that the convex-Delaunay graph (i.e., where the disk is replaced by an arbitrary convex shape) is a c-spanner where the constant c depends only on the perimeter and width of the convex shape.

As for Hamiltonicity in convex shape Delaunay graphs, not much is known. Bonichon et al. [7] proved that every plane triangulation is Delaunay-realizable where homothets of a triangle act as the empty convex shape. This implies that there exist $DG_\triangle$ graphs that do not contain Hamiltonian paths or cycles. Biniaz et al. [6] showed that 7-$DG_\triangle$ contains a bottleneck Hamiltonian cycle and that there exist points sets where 5-$DG_\triangle$ does not contain a bottleneck Hamiltonian cycle. Ábrego et al. [2] showed that the $DG_\square$ admits a Hamiltonian path, while Saumell [18] showed that the $DG_\square$ is not necessarily 1-tough, and therefore does not necessarily contain a Hamiltonian cycle.

Results. We generalize the above results by replacing the disk with an arbitrary con-

[1]A graph G is *1-tough* if removing any k vertices from G results in $\leq k$ connected components.
[2]Note that this implies that the standard Delaunay triangulation is the 0-DG.
[3]According to the definition of k-RNG in [9], they showed Hamiltonicity for 20-RNG.

Type of shape $\mathcal{C}$	$k \leq$	$k \geq$	Bottleneck-$k \geq$
Circles	10 [15]	1 [11]	8 [5]
Equilateral triangles	7 [6]	1 [6]	6 [6]
Squares	7 [Thm. 5.3]	1 [18]	3 [Lemma 6.1]
Regular hexagons	11 [Thm. 5.6]	1 [Lemma 7.1]	6 [Lemma 6.2]
Regular octagons	12 [Thm. 5.8]	1 [Lemma 7.1]	-
Regular t-gons (t even, $t \geq 10$)	11 [Thm. 5.7]	-	-
Regular t-gons ($t = 3m$ with m odd, $m \geq 3$)	24 [Thm. 3.7]	1[Thm. 7.2]	-
Point-symmetric convex	15 [Thm. 4.4]	-	-
Arbitrary convex	24 [Thm. 3.7]	-	-

Table 1: Bounds on the minimum k for which k-$DG_{\mathcal{C}}(S)$ is Hamiltonian and for which k-$GG_{\mathcal{C}}(S)$ contains a $d_{\mathcal{C}}-$bottleneck Hamiltonian cycle.

vex shape $\mathcal{C}$. We show that the k-Gabriel graph, and hence also the k-Delaunay graph, is Hamiltonian for any convex shape $\mathcal{C}$ when $k \geq 24$. Furthermore, we give improved bounds for point-symmetric shapes, as well as for even-sided regular polygons. Table 1 summarizes the bounds obtained. Finally, we provide some lower bounds on the existence of a Hamiltonian cycle for an infinite family of regular polygons, and bottleneck Hamiltonian cycles for the particular cases of hexagons and squares. Together with the results of Bose et al. [8], our results are the first results on graph-theoretic properties of generalized Delaunay graphs that apply to arbitrary convex shapes.

Our results rely on the use of normed metrics and packing lemmas. In fact, in contrast to previous work on Hamiltonicity for generalized Delaunay graphs, our results are the first to use properties of normed metrics to obtain simple proofs for various convex shape Delaunay graphs.

2 Convex distances and the $\mathcal{C}$-Gabriel graph

Let p and q be two points in the plane. Let $\mathcal{C}$ be a compact convex set that contains the origin, denoted $\bar{o}$, in its interior. We denote *the boundary of* $\mathcal{C}$ by $\partial\mathcal{C}$. The *convex distance* $d_{\mathcal{C}}(p,q)$ is defined as follows: If $p = q$, then $d_{\mathcal{C}}(p,q) = 0$. Otherwise, let $\mathcal{C}_p$ be the convex set $\mathcal{C}$ translated by the vector $\overrightarrow{p}$ and let q' be the intersection of the ray from p through q and $\partial\mathcal{C}_p$. Then, $d_{\mathcal{C}}(p,q) = \frac{d(p,q)}{d(p,q')}$ (see Fig. 1) where d denotes the Euclidean distance.

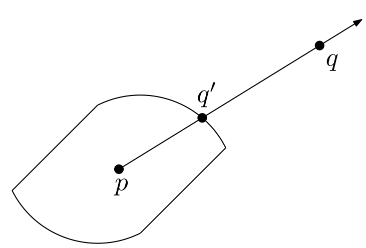

Figure 1: Convex distance from p to q.

The convex set $\mathcal{C}$ is the *unit $\mathcal{C}$-disk* of $d_{\mathcal{C}}$ with center $\bar{o}$, i.e., every point p in $\mathcal{C}$ satisfies that $d_{\mathcal{C}}(\bar{o},p) \leq 1$. The *$\mathcal{C}$-disk with center c and radius r* is defined as the homothet of $\mathcal{C}$ centered at c and with scaling factor r. The *triangle inequality* holds: $d_{\mathcal{C}}(p,q) \leq d_{\mathcal{C}}(p,z) + d_{\mathcal{C}}(z,q), \forall p,q,z \in \mathbb{R}^2$. However, this distance may not define a metric when $\mathcal{C}$ is not *point-symmetric* about

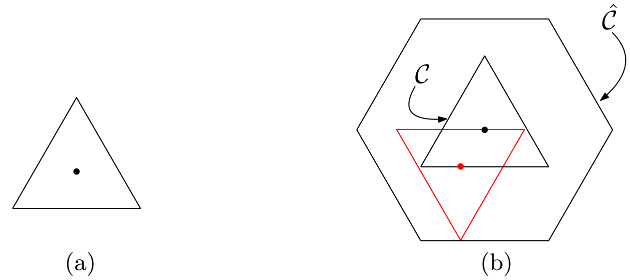

Figure 2: (a) A triangle is a non-symmetric shape $\mathcal{C}$. (b) $\hat{\mathcal{C}}$ for this triangle is a hexagon.

the origin,[4] since there may be points p, q for which $d_{\mathcal{C}}(p,q) \neq d_{\mathcal{C}}(q,p)$. When $\mathcal{C}$ is point-symmetric with respect to the origin, $d_{\mathcal{C}}$ is called a *symmetric convex distance function* and it is a metric. We will refer to such distance functions as *symmetric convex*. Moreover, $d_{\mathcal{C}}(\bar{o}, p)$ defines a *norm*[5] of a *metric space*. In addition, if a point p is on the line segment ab, then $d_{\mathcal{C}}(a,b) = d_{\mathcal{C}}(a,p) + d_{\mathcal{C}}(p,b)$ (see [3, Chapter 7]).

Let S be a set of points in the plane satisfying the following general position assumption: For each pair $p, q \in S$, any minimum homothet of $\mathcal{C}$ having p and q on its boundary does not contain any other point of S on its boundary. The *k-order $\mathcal{C}$-Delaunay graph* of S, denoted k-$DG_{\mathcal{C}}(S)$, is the graph with vertex set S such that, for each pair of points $p, q \in S$, the edge pq is in k-$DG_{\mathcal{C}}(S)$ if there exists a $\mathcal{C}$-disk that has p and q on its boundary and contains at most k points of S different from p and q. When $k = 0$ and $\mathcal{C}$ is a circle, k-$DG_{\mathcal{C}}(S)$ is the standard *Delaunay triangulation*.

The definition of Gabriel graphs requires the notion of a smallest homothet containing two points on its boundary. To be able to use our techniques, it is convenient to be able to associate a distance to the size of such smallest homothets, but $d_{\mathcal{C}}$ fails on defining such distance because $d_{\mathcal{C}}$ might not be symmetric when the shape is not point-symmetric. To circumvent this isssue, Aurenhammer and Paulini [4] showed how to define, from any convex shape $\mathcal{C}$, another shape that results in a distance function that is always symmetric: The set $\hat{\mathcal{C}}$ is defined as the Minkowski sum[6] of $\mathcal{C}$ and its shape reflected about its center. For an example, see Fig. 2. The shape $\hat{\mathcal{C}}$ is point-symmetric and the $d_{\hat{\mathcal{C}}}$-distance from p to q is given by the scaling factor of a smallest homothet of $\mathcal{C}$ containing p and q on its boundary. The diameter and width of $\hat{\mathcal{C}}$ is twice the diameter and width of $\mathcal{C}$, respectively. Moreover, if $\mathcal{C}$ is point-symmetric, $d_{\hat{\mathcal{C}}}(p,q) = \frac{d_{\mathcal{C}}(p,q)}{2}$.

We define the *k-order $\mathcal{C}$-Gabriel graph* of S, denoted k-$GG_{\mathcal{C}}(S)$, as the graph with vertex set S such that, for every pair of points $p, q \in S$, the edge pq is in k-$GG_{\mathcal{C}}(S)$ if and only if there exists a $\mathcal{C}$-disk with radius $d_{\hat{\mathcal{C}}}(p,q)$ that has p and q on its boundary and contains at most k points of S different from p and q. From the definition of k-$GG_{\mathcal{C}}(S)$ and k-$DG_{\mathcal{C}}(S)$ we note that k-$GG_{\mathcal{C}}(S) \subseteq k$-$DG_{\mathcal{C}}(S)$, and it can be a proper subgraph. See Fig. 3a for an example. Further, $\hat{\mathcal{C}}$ always contains $\mathcal{C}$ in its interior. However, for some non point-symmetric convex $\mathcal{C}$ it is not true that $GG_{\hat{\mathcal{C}}} \subseteq GG_{\mathcal{C}}$; see Fig. 3b for an example.

[4]A shape $\mathcal{C}$ is point-symmetric with respect to a point $x \in \mathcal{C}$ provided that for every point $p \in \mathcal{C}$ there is a corresponding point $q \in \mathcal{C}$ such that $pq \in \mathcal{C}$ and x is the midpoint of pq.

[5]A function $\rho(x)$ is a norm if: (a) $\rho(x) = 0$ if and only if $x = \bar{o}$, (b) $\rho(\lambda x) = |\lambda|\rho(x)$ where $\lambda \in \mathbb{R}$, and (c) $\rho(x+y) \leq \rho(x) + \rho(y)$

[6]The Minkowski sum of two sets A and B is defined as $A \oplus B = \{a + b : a \in A, b \in B\}$.

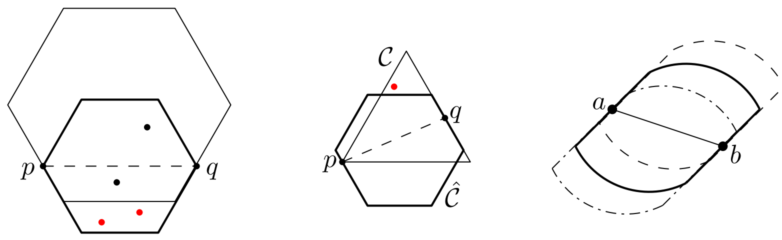

Figure 3: (a) $\mathcal{C}$ is a regular hexagon. Edge pq is in 2-$DG_{\mathcal{C}}(S)$ but it is not in 2-$GG_{\mathcal{C}}(S)$. (b) Edge pq is in $GG_{\hat{\mathcal{C}}}(S)$ but it is not in $GG_{\mathcal{C}}(S)$. (c) Many $\mathcal{C}$-disks $\mathcal{C}(a,b)$ may exist for a and b.

3 Hamiltonicity for general convex shapes

In this section we show that the 24-order $\mathcal{C}$-Gabriel graph is Hamiltonian for any point set S in general position.

For simplicity, denote by $\mathcal{C}_r(a,b)$ a $\mathcal{C}$-disk of radius r with the points a and b on its boundary. For the special case of a *diametral disk*, i.e., when $r = d_{\hat{\mathcal{C}}}(a,b)$, we denote it by $\mathcal{C}(a,b)$. Note that $\mathcal{C}(a,b)$ may not be unique, see Fig. 3c. In addition, we denote by $D_{\mathcal{C}}(c,r)$ the $\mathcal{C}$-disk centered at point c with radius r.

Let $\mathcal{H}$ be the set of all Hamiltoninan cycles of the point set S. Define the $d_{\hat{\mathcal{C}}}$-length sequence of $h \in \mathcal{H}$, denoted $ds_{\mathcal{C}}(h)$, as a sequence of edges of h sorted in decreasing order with respect to the $d_{\hat{\mathcal{C}}}$-metric. Sort the elements of $\mathcal{H}$ in lexicographic order with respect to their $d_{\hat{\mathcal{C}}}$-length sequence, breaking ties arbitrarily. This order is strict. For $h_1, h_2 \in \mathcal{H}$, if h_1 is smaller than h_2 in this order, we write $h_1 \prec h_2$.

Let h be the minimum element in $\mathcal{H}$, often called *bottleneck Hamiltonian cycle*. The approach we follow to prove our bounds, which is similar to the approach in [1, 9, 15], is to show that h is contained in k-$GG_{\mathcal{C}}(S)$ for a small value of k. The strategy for proving that h is contained in 24-$GG_{\mathcal{C}}(S)$ is to show that for every edge $ab \in h$ there are at most 24 points in the interior of any $\mathcal{C}(a,b)$. In order to do this, we associate each point in the interior of an arbitrary fixed $\mathcal{C}(a,b)$ to another point. Later, we show that the $d_{\hat{\mathcal{C}}}$-distances between such associated points and a is at least $d_{\hat{\mathcal{C}}}(a,b)$. Finally, we use a packing argument to show that there are at most 24 associated points, which leads to a maximum of 24 points contained in $\mathcal{C}(a,b)$.

Let $ab \in h$; we assume without loss of generality that $d_{\hat{\mathcal{C}}}(a,b) = 1$. Let $U = \{u_1, u_2, \ldots, u_k\}$ be the set of points in S different from a and b that are in the interior of an arbitrary fixed $\mathcal{C}(a,b)$.[7] When traversing h from b to a, we visit the points of U in the order $u_1, \ldots, u_k$. For each point u_i, define s_i to be the point preceding u_i in h. See Fig. 4a.

Note that if a point p is in the interior of $\mathcal{C}(a,b)$, then for any q on the boundary of $\mathcal{C}(a,b)$ there exists a $\mathcal{C}$-disk (not necessarily diametral) through p and q contained in $\mathcal{C}(a,b)$. Moreover, any diametral disk through p and q has size smaller than or equal to the size of this $\mathcal{C}$-disk. Therefore, $d_{\hat{\mathcal{C}}}(a,u_i) < 1$ and $d_{\hat{\mathcal{C}}}(b,u_i) < 1$ for any $i \in \{1,\ldots,k\}$. Furthermore, we have the following:

Claim 3.1. *Let $1 \le i \le k$. Then* $d_{\hat{\mathcal{C}}}(a,s_i) \ge \max\{d_{\hat{\mathcal{C}}}(s_i,u_i), 1\}$

[7] Since S is in general position, only a and b can lie on the boundary of $\mathcal{C}(a,b)$.

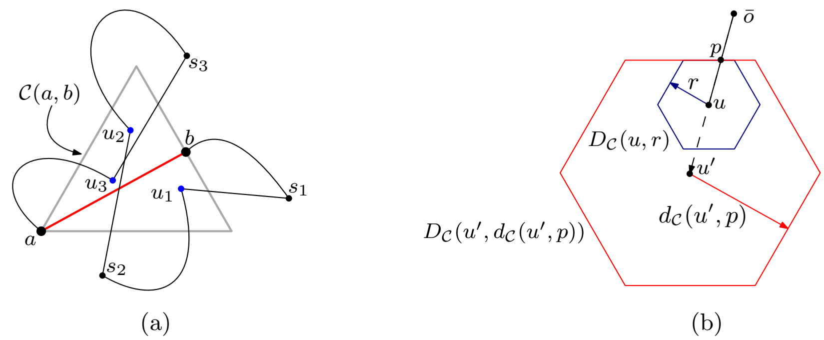

Figure 4: (a) Example of U in $\mathcal{C}(a,b)$. (b) $D_{\mathcal{C}}(u,r)$ is contained in $D_{\mathcal{C}}(u', d_{\mathcal{C}}(u',p))$ where $u' = \lambda u$ with $\lambda > 1$.

Proof. If $s_1 = b$, then $d_{\hat{\mathcal{C}}}(a, s_1) = 1$ and $d_{\hat{\mathcal{C}}}(s_1, u_1) < 1$. Otherwise, define $h'{=}(h \setminus \{ab, s_i u_i\}) \cup \{a s_i, u_i b\}$. For sake of a contradiction suppose that $d_{\hat{\mathcal{C}}}(a, s_i){<}\max\{d_{\hat{\mathcal{C}}}(s_i, u_i), 1\}$. It holds that $d_{\hat{\mathcal{C}}}(a, s_i) < \max\{d_{\hat{\mathcal{C}}}(s_i, u_i), d_{\hat{\mathcal{C}}}(a, b)\}$ since $d_{\hat{\mathcal{C}}}(a, b) = 1$. Also, $d_{\hat{\mathcal{C}}}(u_i, b) < 1$ since $u_i \in \mathcal{C}(a, b)$. Thus, $\max\{d_{\hat{\mathcal{C}}}(a, s_i), d_{\hat{\mathcal{C}}}(u_i, b)\} < \max\{d_{\hat{\mathcal{C}}}(s_i, u_i), d_{\hat{\mathcal{C}}}(a, b)\}$. Therefore $h' \prec h$, which contradicts the definition of h. □

Claim 3.1 implies that, for each $i \in \{1, \ldots, k\}$, s_i is not in the interior of $\mathcal{C}(a, b)$.

Claim 3.2. *Let $1 \leq i < j \leq k$. Then $d_{\hat{\mathcal{C}}}(s_i, s_j) \geq \max\{d_{\hat{\mathcal{C}}}(s_i, u_i), d_{\hat{\mathcal{C}}}(s_j, u_j), 1\}$.*

Proof. For sake of a contradiction suppose that $d_{\hat{\mathcal{C}}}(s_i, s_j) < \max\{d_{\hat{\mathcal{C}}}(s_i, u_i),\ d_{\hat{\mathcal{C}}}(s_j, u_j), 1\}$. Consider the Hamiltonian cycle $h' = h \setminus \{(a, b), (s_i, u_i), (s_j, u_j)\} \cup \{(s_i, s_j), (u_i, a), (u_j, b)\}$. As in Claim 3.1 we have that $d_{\hat{\mathcal{C}}}(u_i, a) < 1$ and $d_{\hat{\mathcal{C}}}(u_j, b) < 1$. So, $\max\{d_{\hat{\mathcal{C}}}(s_i, s_j), d_{\hat{\mathcal{C}}}(u_i, a), d_{\hat{\mathcal{C}}}(u_j, b)\} < \max\{d_{\hat{\mathcal{C}}}(s_i, u_i),\ d_{\hat{\mathcal{C}}}(s_j, u_j),\ d_{\hat{\mathcal{C}}}(a, b)\}$. Therefore, $h' \prec h$ which contradicts the minimality of h. □

The $d_{\mathcal{C}}$*-distance from a point* v to a region C is given by the minimum $d_{\mathcal{C}}$-distance from v to any point u in C.

Observation 3.3. *Let $u \notin D_{\mathcal{C}}(\bar{o}, r)$ for some $r \in \mathbb{R}^+$ and let p be the intersection point of $\partial D_{\mathcal{C}}(\bar{o}, r))$ and line segment $\bar{o}u$. Then, the $d_{\mathcal{C}}$-distance from u to $D_{\mathcal{C}}(\bar{o}, r)$ is $d_{\mathcal{C}}(u, p)$.*

Proof. Since p is in $\partial D_{\mathcal{C}}(\bar{o}, r)$ and $u \notin D_{\mathcal{C}}(\bar{o}, r)$, $u = \lambda p$ for some $\lambda > 1 \in \mathbb{R}$. In addition, the $d_{\mathcal{C}}$-distance from u to $D_{\mathcal{C}}(\bar{o}, r)$ is at least $d_{\mathcal{C}}(u, p)$. For the sake of a contradiction suppose that the $d_{\mathcal{C}}$-distance from u to $D_{\mathcal{C}}(\bar{o}, r)$ is less than $d_{\mathcal{C}}(u, p)$. Thus, there exists a point $v \in \partial D_{\hat{\mathcal{C}}}(\bar{o}, r)$ such that $d_{\hat{\mathcal{C}}}(u, v) < d_{\hat{\mathcal{C}}}(u, p)$, and $r\lambda = d_{\hat{\mathcal{C}}}(\bar{o}, u) \leq d_{\hat{\mathcal{C}}}(\bar{o}, v) + d_{\hat{\mathcal{C}}}(v, u) < d_{\hat{\mathcal{C}}}(\bar{o}, v) + d_{\hat{\mathcal{C}}}(p, u) = r + r\lambda - r = r\lambda$, which is a contradiction. □

Without loss of generality assume that a is the origin $\bar{o}$. Since for any point u in $\mathcal{C}(a, b)$, $d_{\hat{\mathcal{C}}}(\bar{o}, u) = d_{\hat{\mathcal{C}}}(a, u) \leq 1$, we have that $D_{\hat{\mathcal{C}}}(\bar{o}, 1)$ contains $\mathcal{C}(a, b)$. Also, from Claim 3.1, we have that s_i is not in the interior of $D_{\hat{\mathcal{C}}}(\bar{o}, 1)$ for all $i \in \{1, \ldots, k\}$. Let $D_{\hat{\mathcal{C}}}(\bar{o}, 2)$ be the $\hat{\mathcal{C}}$-disk centered at $\bar{o} = a$ with radius 2. For each $s_i \notin D_{\hat{\mathcal{C}}}(\bar{o}, 2)$, define s'_i as the intersection of $\partial D_{\hat{\mathcal{C}}}(\bar{o}, 2)$ with the ray $\overrightarrow{\bar{o}s_i}$. Let $s'_i = s_i$ when s_i is inside $D_{\hat{\mathcal{C}}}(\bar{o}, 2)$. See Fig. 5.

Observation 3.4. *If $s_j \notin D_{\hat{\mathcal{C}}}(\bar{o}, 2)$ (with $1 \leq j \leq k$), the $d_{\hat{\mathcal{C}}}$-distance from s'_j to $D_{\hat{\mathcal{C}}}(\bar{o}, 1)$ is 1.*

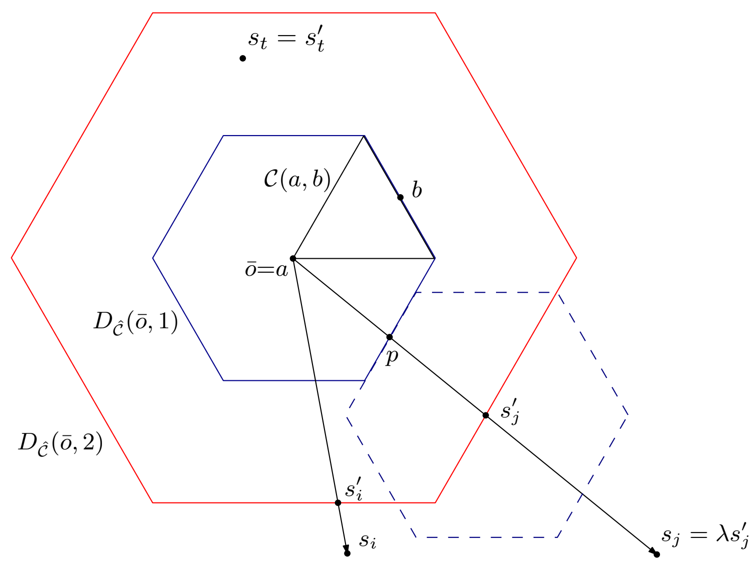

Figure 5: $\mathcal{C}(a,b)$ has radius 1, $D_{\hat{\mathcal{C}}}(\bar{o},1)$ is the $\hat{\mathcal{C}}$-disk with radius 1 centered at $\bar{o}$ and $D_{\hat{\mathcal{C}}}(\bar{o},2)$ is the $\hat{\mathcal{C}}$-disk with radius 2 centered at $\bar{o}$. The points s'_i and s'_j are projections of s_i and s_j on $\partial D_{\hat{\mathcal{C}}}(\bar{o},2)$, respectively. The dashed $\hat{\mathcal{C}}$-disk is centered at s'_j and has radius 1.

Proof. Since $s_j \notin D_{\hat{\mathcal{C}}}(\bar{o},2)$, s'_j is on the boundary of $D_{\hat{\mathcal{C}}}(\bar{o},2)$ and $d_{\hat{\mathcal{C}}}(\bar{o},s'_j)=2$. Let p be the intersection point of $\partial D_{\hat{\mathcal{C}}}(\bar{o},1)$ and $\bar{o}s_j$. Then $d_{\hat{\mathcal{C}}}(\bar{o},p)=1$. By Observation 3.3 the $d_{\hat{\mathcal{C}}}$-distance from s'_j to $D_{\hat{\mathcal{C}}}(\bar{o},1)$ is $d_{\hat{\mathcal{C}}}(s'_j,p)=d_{\hat{\mathcal{C}}}(p,s'_j)=d_{\hat{\mathcal{C}}}(\bar{o},s'_j)-d_{\hat{\mathcal{C}}}(\bar{o},p)=2-1=1$. □

The following claim is needed to prove our key lemma. Intuitively, this claim shows that if there is a point-symmetric $\mathcal{C}$-disk C of radius r centered at a point u such that $r \le d_{\mathcal{C}}(u,\bar{o})$, then C is contained in any $\mathcal{C}$-disk with $\partial C \cap \overrightarrow{\bar{o}u}$ on its boundary such that its center u' lies on the ray $\bar{o}u$ and is farther to $\bar{o}$ than u. For an example, see Fig. 4b.

Claim 3.5. *Let $\mathcal{C}$ be a point-symmetric convex shape. Let u be a point in the plane different from the origin $\bar{o}$. Let $r < d_{\mathcal{C}}(u,\bar{o})$. Let p be the intersection point of $\partial D_{\mathcal{C}}(u,r)$ and line segment $\bar{o}u$. Let $u' = \lambda u$, with $\lambda > 1 \in \mathbb{R}$, be a point defined by vector u scaled by a factor of λ. Then $D_{\mathcal{C}}(u,r) \subset D_{\mathcal{C}}(u',d_{\mathcal{C}}(u',p))$. (See Fig. 4b.)*

Proof. Let $q \in D_{\mathcal{C}}(u,r)$; then $d_{\mathcal{C}}(u,q) \le d_{\mathcal{C}}(u,p)$. Since u is on the line segment $u'p$, we have that $d_{\mathcal{C}}(u',p)=d_{\mathcal{C}}(u',u)+d_{\mathcal{C}}(u,p)$. Hence $d_{\mathcal{C}}(u',q) \le d_{\mathcal{C}}(u',u)+d_{\mathcal{C}}(u,q) \le d_{\mathcal{C}}(u',u)+d_{\mathcal{C}}(u,p)=d_{\mathcal{C}}(u',p)$. Therefore, $D_{\mathcal{C}}(u,r)$ is contained in $D_{\mathcal{C}}(u',d_{\mathcal{C}}(u',p))$. □

Using the previous claims we can prove a key lemma stating that for every pair of points s'_i and s'_j, we have that $d_{\hat{\mathcal{C}}}(s'_i,s'_j) \ge 1$. From this lemma we can conclude that any pair of $\hat{\mathcal{C}}$-disks with radius $\frac{1}{2}$ centered at s'_i and s'_j are internally disjoint, which allows us to bound $|U|$ via a packing argument.

Lemma 3.6. *For any pair s_i and s_j with $i \neq j$, we have that $d_{\hat{\mathcal{C}}}(s'_i,s'_j) \ge 1$.*

Proof. If both s_i and s_j are in $D_{\hat{\mathcal{C}}}(\bar{o},2)$, then from Claim 3.2 we have that $d_{\hat{\mathcal{C}}}(s'_i,s'_j) = d_{\hat{\mathcal{C}}}(s_i,s_j) \ge 1$. Otherwise, we assume, without loss of generality, that $d_{\hat{\mathcal{C}}}(\bar{o},s_j) \ge d_{\hat{\mathcal{C}}}(\bar{o},s_i)$. Then, $s_j \notin D_{\hat{\mathcal{C}}}(\bar{o},2)$. Since s'_j is on the line segment $\bar{o}s_j$, we have $s_j = \lambda s'_j$ for some $\lambda > 1$.

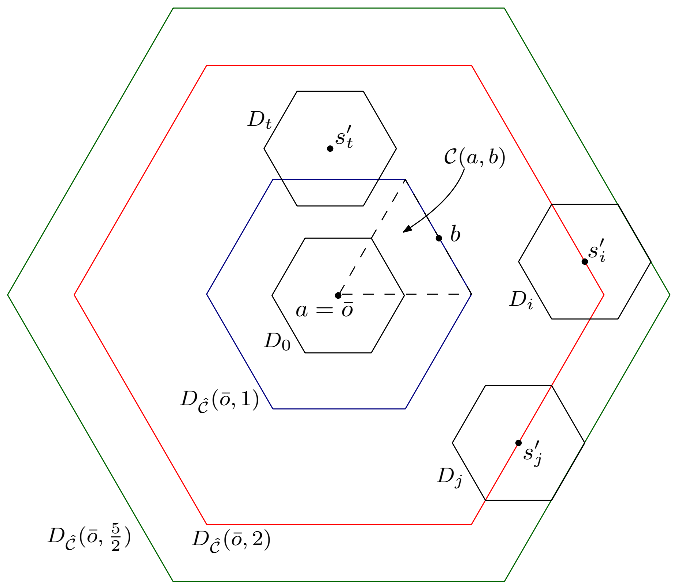

Figure 6: The $\hat{\mathcal{C}}$-disks D_0, D_i, D_j and D_t of radius $\frac{1}{2}$ are centered at a, s'_i, s'_j and s'_t, respectively. Such $\hat{\mathcal{C}}$-disks are contained in the $\hat{\mathcal{C}}$-disk $D_{\hat{\mathcal{C}}}(\bar{o}, \frac{5}{2})$.

Let p be the intersection point of $\partial D_{\hat{\mathcal{C}}}(\bar{o}, 1)$ and $\bar{o}s_j$. Since $d_{\hat{\mathcal{C}}}$ defines a norm, we have $d_{\hat{\mathcal{C}}}(\lambda s'_j, \bar{o}) = \lambda d_{\hat{\mathcal{C}}}(s'_j, \bar{o})$. By Observation 3.4 we have that $d_{\hat{\mathcal{C}}}(s_j, p) = d_{\hat{\mathcal{C}}}(s_j, \bar{o}) - d_{\hat{\mathcal{C}}}(p, \bar{o}) = \lambda d_{\hat{\mathcal{C}}}(s'_j, \bar{o}) - 1 = 2\lambda - 1$. From Observation 3.3 it follows that the $d_{\hat{\mathcal{C}}}$-distance from s_j to $D_{\hat{\mathcal{C}}}(\bar{o}, 1)$ is equal to $d_{\hat{\mathcal{C}}}(s_j, p)$. Further, $d_{\hat{\mathcal{C}}}(s_j, s'_j) = d_{\hat{\mathcal{C}}}(s_j, \bar{o}) - d_{\hat{\mathcal{C}}}(s'_j, \bar{o}) = 2\lambda - 2$. Let us prove that $d_{\hat{\mathcal{C}}}(s'_i, s'_j) \geq 1$. For sake of a contradiction suppose that $d_{\hat{\mathcal{C}}}(s'_i, s'_j) < 1$. Let $D_{s'_j} = D_{\hat{\mathcal{C}}}(s'_j, 1)$. By Observation 3.4, $d_{\hat{\mathcal{C}}}(s'_j, p) = 1$. Therefore, p is on $\partial D_{s'_j}$. Now, we consider two cases:
Case 1) $s_i \in D_{\hat{\mathcal{C}}}(\bar{o}, 2)$. Then $d_{\hat{\mathcal{C}}}(\bar{o}, s_i) \leq 2$. Since $d_{\hat{\mathcal{C}}}(s'_i, s'_j) < 1$, we have $s_i \in D_{s'_j}$. From Claim 3.5 it follows that $D_{s'_j}$ is contained in $D_{\hat{\mathcal{C}}}(s_j, d_{\hat{\mathcal{C}}}(s_j, p))$. Thus, $s'_i \in D_{\hat{\mathcal{C}}}(s_j, d_{\hat{\mathcal{C}}}(s_j, p))$ and $d_{\hat{\mathcal{C}}}(s_j, s'_i) = d_{\hat{\mathcal{C}}}(s_j, s_i) \leq d_{\hat{\mathcal{C}}}(s_j, p)$. Since S is in general position, u_j is in the interior of $D_{\hat{\mathcal{C}}}(\bar{o}, 1)$. Hence, $d_{\hat{\mathcal{C}}}(s_j, s_i) \leq d_{\hat{\mathcal{C}}}(s_j, p) < d_{\hat{\mathcal{C}}}(s_j, u_j)$, which contradicts Claim 3.2.
Case 2) $s_i \notin D_{\hat{\mathcal{C}}}(\bar{o}, 2)$. Then $d_{\hat{\mathcal{C}}}(\bar{o}, s_i) > 2$. Thus, $s_i = \delta s'_i$ for some $\delta > 1 \in \mathbb{R}$. Moreover, since $d_{\hat{\mathcal{C}}}(\bar{o}, s_j) \geq d_{\hat{\mathcal{C}}}(\bar{o}, s_i)$ and s'_i, s'_j are on $\partial D_{\hat{\mathcal{C}}}(\bar{o}, 2)$, $\delta \leq \lambda$. Hence, s_i is on the line segment $s'_i(\lambda s'_i)$. Let $D_{s_j} = D_{\hat{\mathcal{C}}}(s_j, 2\lambda - 1)$. Note that $\lambda < 2\lambda - 1$ because $\lambda > 1$. Since $d_{\hat{\mathcal{C}}}$ defines a norm, $d_{\hat{\mathcal{C}}}(s_j, \lambda s'_i) = d_{\hat{\mathcal{C}}}(\lambda s'_j, \lambda s'_i) = \lambda d_{\hat{\mathcal{C}}}(s'_j, s'_i) < \lambda < 2\lambda - 1$. Hence, $\lambda s'_i \in D_{s_j}$. In addition, since $d_{\hat{\mathcal{C}}}(s_j, p) = 2\lambda - 1$, from Claim 3.5 it follows that $D_{s'_j} \subseteq D_{s_j}$. Therefore, $s'_i \in D_{s_j}$. Thus, the line segment $s'_i(\lambda s'_i)$ is contained in D_{s_j}. Hence, $s_i \in D_{s_j}$. Then, $d_{\hat{\mathcal{C}}}(s_j, s_i) \leq 2\lambda - 1 = d_{\hat{\mathcal{C}}}(s_j, p) < d_{\hat{\mathcal{C}}}(s_j, u_j)$ which contradicts Claim 3.2. □

Theorem 3.7. *For any set S of points in general position and convex shape $\mathcal{C}$, the graph $24\text{-}GG_{\mathcal{C}}(S)$ is Hamiltonian.*

Proof. For each s_i we define the $\hat{\mathcal{C}}$-disk $D_i = D_{\hat{\mathcal{C}}}(s'_i, \frac{1}{2})$. We also set $D_0 := D_{\hat{\mathcal{C}}}(\bar{o}, \frac{1}{2})$ (recall that we can assume without loss of generality that $a = \bar{o}$). By Lemma 3.6, each pair of $\hat{\mathcal{C}}$-disks D_i and D_j $(0 < i < j \leq k)$ are internally disjoint. Note that, if s'_i is on $\partial D_{\hat{\mathcal{C}}}(\bar{o}, 2)$, then D_0 and D_i are internally disjoint. On the other hand, if s'_i is in the interior of $D_{\hat{\mathcal{C}}}(\bar{o}, 2)$, then by definition $s'_i = s_i$. Thus, by Claim 3.1 D_0 is internally disjoint from D_i. See Fig. 6.

Since $s'_i \in D_{\hat{\mathcal{C}}}(\bar{o}, 2)$ for all i, each disk D_i is inside $D_{\hat{\mathcal{C}}}(\bar{o}, \frac{5}{2})$. In $D_{\hat{\mathcal{C}}}(\bar{o}, \frac{5}{2})$, there can be at most $\frac{Area(D_{\hat{\mathcal{C}}}(\bar{o}, \frac{5}{2}))}{Area(D_0)} = \frac{(\frac{5}{2})^2 Area(\hat{\mathcal{C}})}{(\frac{1}{2})^2 Area(\hat{\mathcal{C}})} = 25$ internally disjoint disks of type D_i. Thus, since D_0 is centered at a, there are at most 24 points s'_i in $D_{\hat{\mathcal{C}}}(\bar{o}, 1)$. As a consequence, there are at most 24 points of S in the interior of $\mathcal{C}(a, b)$, and the bottleneck Hamiltonian cycle of S is contained in 24-$GG_{\mathcal{C}}(S)$. □

4 Hamiltonicity for point-symmetric convex shapes

In this section we improve Theorem 3.7 for the case where $\mathcal{C}$ is convex and point-symmetric. We use similar arguments to those in Section 3.

Consider h defined as before, i.e., h is the minimum Hamiltonian cycle in $\mathcal{H}$. Let ab be an edge in h and consider an arbitrary fixed $\mathcal{C}(a, b)$. In this section it will be more convenient to assume without loss of generality that $d_{\mathcal{C}}(a, b) = 2$ and that $\mathcal{C}(a, b)$ is centered at the origin $\bar{o}$. Thus, $\mathcal{C}(a, b) = D_{\mathcal{C}}(\bar{o}, 1)$, see Fig. 7. Consider again the set $U = \{u_1, \ldots, u_k\}$ defined as in Section 3, and let s_i be the predecessor of u_i in h.

Using that $d_{\mathcal{C}}(a, b) = 2d_{\hat{\mathcal{C}}}(a, b)$ when $\mathcal{C}$ is point-symmetric, we can prove the following claims.

Claim 4.1. *$d_{\mathcal{C}}(s_i, a) \geq \max\{d_{\mathcal{C}}(s_i, u_i), 2\}$.*

Proof. By Claim 3.1 we have that $d_{\mathcal{C}}(s_i, a) = 2d_{\hat{\mathcal{C}}}(s_i, a) \geq 2\max\{d_{\hat{\mathcal{C}}}(s_i, u_i), 1\} = \max\{2d_{\hat{\mathcal{C}}}(s_i, u_i), 2\} = \max\{d_{\mathcal{C}}(s_i, u_i), 2\}$. □

Claim 4.2. *Let $1 \leq i < j \leq k$, then $d_{\mathcal{C}}(s_i, s_j) \geq \max\{d_{\mathcal{C}}(s_i, u_i), d_{\mathcal{C}}(s_j, u_j), 2\}$.*

Proof. By Claim 3.2 we have that $d_{\mathcal{C}}(s_i, s_j) = 2d_{\hat{\mathcal{C}}}(s_i, s_j) \geq 2\max\{d_{\hat{\mathcal{C}}}(s_i, u_i), d_{\hat{\mathcal{C}}}(s_j, u_j), 1\} = \max\{2d_{\hat{\mathcal{C}}}(s_i, u_i), 2d_{\hat{\mathcal{C}}}(s_j, u_j), 2\} = \max\{d_{\mathcal{C}}(s_i, u_i), d_{\mathcal{C}}(s_j, u_j), 2\}$. □

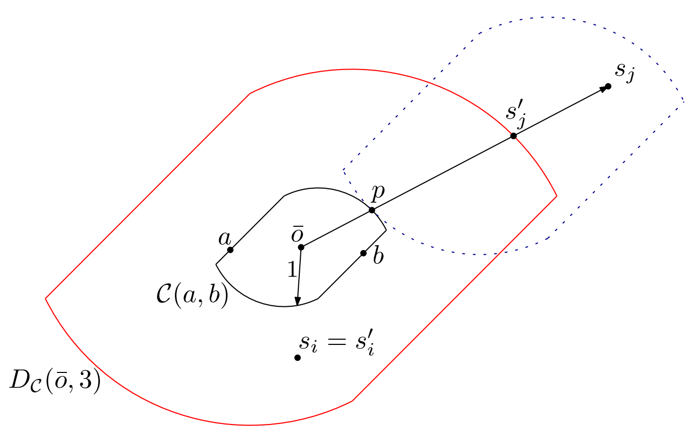

Figure 7: $\mathcal{C}(a, b)$ has radius 1 and it is centered at $\bar{o}$. The point s_j is not in $D_{\mathcal{C}}(\bar{o}, 3)$, so s'_j is the intersection point of $\bar{o}s_j \cap \partial D_{\mathcal{C}}(\bar{o}, 3)$. The dotted $\mathcal{C}$-disk is centered at s'_j and has radius 2.

From Claim 4.1, we have that s_i is not in the interior of $D_{\mathcal{C}}(\bar{o}, 1) = \mathcal{C}(a, b)$ for all $i \in \{1, \ldots, k\}$. Let $D_{\mathcal{C}}(\bar{o}, 3)$ be the $\mathcal{C}$-disk centered at $\bar{o}$ with radius 3. For each $s_i \notin D_{\mathcal{C}}(\bar{o}, 3)$, define s'_i as the intersection of $\partial D_{\mathcal{C}}(\bar{o}, 3)$ with the ray $\overrightarrow{\bar{o}s_i}$. We let $s'_i = s_i$ when s_i is inside $D_{\mathcal{C}}(\bar{o}, 3)$. See Figure 7.

The following lemma is similar to Lemma 3.6. We show that every pair s'_i and s'_j are at $d_{\mathcal{C}}$-distance at least 2. This lemma allows us again to reduce our problem to a packing problem.

Lemma 4.3. *For any pair s_i and s_j with $i \neq j$, we have that $d_{\mathcal{C}}(s'_i, s'_j) \geq 2$. Moreover, if at least one of s_i and s_j is not in $D_{\mathcal{C}}(\bar{o}, 3)$, then $d_{\mathcal{C}}(s'_i, s'_j) > 2$.*

Proof. If both s_i and s_j are in $D_{\mathcal{C}}(\bar{o}, 3)$, then from Claim 4.2 we have that $d_{\mathcal{C}}(s'_i, s'_j) = d_{\mathcal{C}}(s_i, s_j) \geq 2$. Otherwise, assume without loss of generality that $d_{\mathcal{C}}(\bar{o}, s_j) \geq d_{\mathcal{C}}(\bar{o}, s_i)$. Then $s_j \notin D_{\mathcal{C}}(\bar{o}, 3)$ and s'_j is on the line segment $\bar{o}s_j$. Thus, $s_j = \lambda s'_j$ for some $\lambda > 1$. Let p be the intersection point of $\partial\mathcal{C}(a, b)$ and $\bar{o}s_j$. By Observation 3.3 the $d_{\mathcal{C}}$-distance from s'_j to $\mathcal{C}(a, b)$ is $d_{\mathcal{C}}(s'_j, p) = d_{\mathcal{C}}(s'_j, \bar{o}) - d_{\mathcal{C}}(p, \bar{o}) = 2$. Since $d_{\mathcal{C}}$ defines a norm, $d_{\mathcal{C}}(s_j, p) = d_{\mathcal{C}}(s_j, \bar{o}) - d_{\mathcal{C}}(p, \bar{o}) = \lambda d_{\mathcal{C}}(s'_j, \bar{o}) - 1 = 3\lambda - 1$, and this corresponds to the $d_{\mathcal{C}}$-distance from s_j to $\mathcal{C}(a, b)$. Further, $d_{\mathcal{C}}(s_j, s'_j) = d_{\mathcal{C}}(s_j, \bar{o}) - d_{\mathcal{C}}(s'_j, \bar{o}) = 3\lambda - 3$. For sake of contradiction we suppose that $d_{\mathcal{C}}(s'_i, s'_j) \leq 2$. Thus, s'_i is in $D_{\mathcal{C}}(s'_j, 2)$. We consider the following two cases.
Case 1) $s_i \in D_{\mathcal{C}}(\bar{o}, 3)$. Then $d_{\mathcal{C}}(\bar{o}, s_i) \leq 3$. Since $d_{\mathcal{C}}(s'_i, s'_j) \leq 2$, $s_i = s'_i \in D_{\mathcal{C}}(s'_j, 2)$. From Claim 3.5 follows that $D_{\mathcal{C}}(s'_j, 2) \subset D_{\mathcal{C}}(s_j, 3\lambda - 1)$. Thus, $s_i \in D_{\mathcal{C}}(s_j, 3\lambda - 1)$. Hence, $d_{\mathcal{C}}(s_j, s'_i) = d_{\mathcal{C}}(s_j, s_i) \leq d_{\mathcal{C}}(s_j, p)$. Since S is in general position, u_j is in the interior of $\mathcal{C}(a, b)$. Therefore, $d_{\mathcal{C}}(s_j, s_i) \leq d_{\mathcal{C}}(s_j, p) < d_{\mathcal{C}}(s_j, u_j)$, which contradicts Claim 4.2.
Case 2) $s_i \notin D_{\mathcal{C}}(\bar{o}, 3)$. Then $s'_i \in \partial D_{\mathcal{C}}(\bar{o}, 3)$ and $s_i = \delta s'_i$ for some $\delta > 1$. Moreover, since $d_{\mathcal{C}}(\bar{o}, s_j) \geq d_{\mathcal{C}}(\bar{o}, s_i)$ and s'_i, s'_j are on the boundary of $D_{\mathcal{C}}(\bar{o}, 3)$, $\delta \leq \lambda$. Hence, s_i is on the line segment $s'_i(\lambda s'_i)$. Note that $2\lambda < 3\lambda - 1$ because $\lambda > 1$. Since $d_{\mathcal{C}}$ defines a norm, $d_{\mathcal{C}}(s_j, \lambda s'_i) = \lambda d_{\mathcal{C}}(s'_j, s'_i) \leq 2\lambda < 3\lambda - 1$. Hence, $\lambda s'_i \in D_{\mathcal{C}}(s_j, 3\lambda - 1)$. In addition, from Claim 3.5 it follows that $D_{\mathcal{C}}(s'_j, 2) \subseteq D_{\mathcal{C}}(s_j, 3\lambda - 1)$. Thus, $s'_i \in D_{\mathcal{C}}(s_j, 3\lambda - 1)$ and the line segment $s'_i(\lambda s'_i)$ is contained in $D_{\mathcal{C}}(s_j, 3\lambda - 1)$. Then, $s_i \in D_{\mathcal{C}}(s_j, 3\lambda - 1)$ and $d_{\mathcal{C}}(s_j, s_i) \leq 3\lambda - 1 = d_{\mathcal{C}}(s_j, p) < d_{\mathcal{C}}(s_j, u_j)$, which contradicts Claim 4.2. □

Theorem 4.4. *For any set S of points in general position and point-symmetric convex shape $\mathcal{C}$, the graph 15-$GG_{\mathcal{C}}(S)$ is Hamiltonian.*

Proof. For each $s_i \in S$ we define the $\mathcal{C}$-disk $D_i = D_{\mathcal{C}}(s'_i, 1)$. We also set $D_0 := D_{\mathcal{C}}(a, 1)$. From Lemma 4.3, each pair of $\mathcal{C}$-disks D_i and D_j are internally disjoint, for $0 < i < j \leq k$. Note that, if s'_i is on $\partial D_{\mathcal{C}}(\bar{o}, 3)$, then D_0 and D_i are internally disjoint. On the other hand, if s'_i is in the interior of $D_{\mathcal{C}}(\bar{o}, 3)$, then by definition $s'_i = s_i$. Thus, by Claim 4.1 D_0 is internally disjoint from D_i. Consider $D_{\mathcal{C}}(\bar{o}, 4)$. Since, $s'_i \in D_{\mathcal{C}}(\bar{o}, 3)$ for all $i \in \{1, \ldots k\}$, then each disk D_i is inside $D_{\mathcal{C}}(\bar{o}, 4)$. Hence, in $D_{\mathcal{C}}(\bar{o}, 4)$ there can be at most $\frac{Area(D_{\mathcal{C}}(\bar{o},4))}{Area(\mathcal{C})} = \frac{4^2 Area(\mathcal{C})}{Area(\mathcal{C})} = 16$ internally disjoint disks of type D_i. Since D_0 is centered at a, there are at most 15 points s'_i in $D_{\mathcal{C}}(\bar{o}, 3)$. Therefore, there are at most 15 points of S in $\mathcal{C}(a, b)$, and the bottleneck Hamiltonian cycle of S is contained in 15-$GG_{\mathcal{C}}(S)$. □

5 Hamiltonicity for regular polygons

An important family of point-symmetric convex shapes is that of regular even-sided polygons. When $\mathcal{C}$ is a regular polygon $\mathcal{P}_t$ with t sides, for t even, we can improve the previous bound by analyzing the properties of the shape for different values of t.

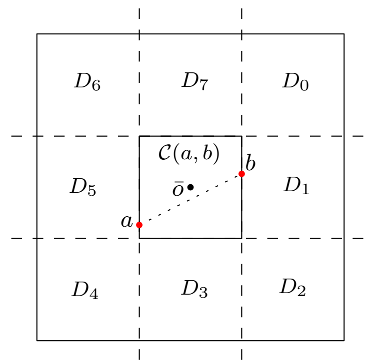

Figure 8: Lines $x = -1, x = 1, y = -1$, and $y = 1$ split $D_\Box(3, \bar{o})$ into nine unit squares: $\mathcal{C}(a, b), D_0, \ldots, D_7$.

5.1 Hamiltonicity for squares

First, we consider the case when the polygon is a square. In this case, we divide $D_\Box(\bar{o}, 3)$ into 9 disjoint squares of radius 1 and show that there can be at most one point of $\{a, s'_1, \ldots, s'_k\}$ in each such square. We use lines $x = -1, x = 1, y = -1$, and $y = 1$ to split $D_\Box(\bar{o}, 3)$ into 9 squares of radius 1. Refer to Fig. 8. Let $D_0, D_1, \ldots, D_7$ be the squares of radius 1 in $D_\Box(\bar{o}, 3)$ different from $C(a, b)$, ordered clockwise, and where D_0 is the top-right corner square. In the following lemma we prove that there is at most one point of $\{a, s'_1, \ldots, s'_k\}$ in each D_i. Let indices be taken modulo 8. Note that each D_i shares a side with D_{i-1}, and for each odd i, D_i shares a side with $\mathcal{C}(a, b)$. Moreover, there exists a D_i that contains a on its boundary. We will associate any point in $D_\Box(\bar{o}, 3)$ (not in the interior of $\mathcal{C}(a, b)$) to a unique square D_i in the following way: Let p be a point in D_i. If p does not lie on the shared boundary of D_i and some other D_j, then p is associated to D_i. If i is odd and p is the intersection point $D_i \cap D_{i-1} \cap D_{i-2}$, then p is associated to D_{i-2} (p can be a or b). Otherwise, if p is on the edge $D_i \cap D_{i-1}$, then p is associated to D_{i-1}.

Observation 5.1. *Any two points at $d_\Box$-distance 2 in a unit square must be on opposite sides of the square.*

Lemma 5.2. *There is at most one s'_j associated to each D_i. Moreover, the D_i containing the point a on its boundary has no s'_j associated to it.*

Proof. Suppose that there are two points s'_j and s'_m associated to D_i. From Lemma 4.3 we have that $d_\Box(s'_j, s'_m) \geq 2$. Also, since D_i is a unit square, $d_\Box(s'_j, s'_m) \leq 2$. Therefore, $d_\Box(s'_j, s'_m) = 2$. Then Lemma 4.3 implies that s_j and s_m must be inside $D_\mathcal{C}(\bar{o}, 3)$. In addition, by Observation 5.1, the points s_j and s_m are on opposite sides of the boundary of D_i. For simplicity we will assume that $d_\Box(\bar{o}, s_j) \geq d_\Box(\bar{o}, s_m)$. If i is even, then the $d_\Box$-distance of s_j to $\mathcal{C}(a, b)$ is exactly 2. We refer to Fig. 9a and 9b. Recall that, by our general position assumption, u_j is in the interior of $\mathcal{C}(a, b)$. Thus, the $d_\Box$-distance from s_j to $\mathcal{C}(a, b)$ is less than $d_\Box(s_j, u_j)$, i.e., $d_\Box(s_j, u_j) > 2$. Hence, $d_\Box(s_j, s_m) = 2 < d_\Box(s_j, u_j)$ which contradicts Claim 4.2. Therefore, if i is even, there is at most one point in D_i, which is associated to it. If i is odd, then s_j is either on $D_i \cap D_{i-1}$ or $D_i \cap D_{i+1}$, or on $D_i \cap \partial D_\mathcal{C}(\bar{o}, 3)$ (see Fig. 9c and 9d). If s_j is on $D_i \cap D_{i-1}$ or $D_i \cap D_{i+1}$, then only one of s_j and s_m is associated to D_i. If s_j is on $D_i \cap \partial D_\mathcal{C}(\bar{o}, 3)$, then by Observation 5.1, s_m is on $\mathcal{C}(a, b)$, which by our general

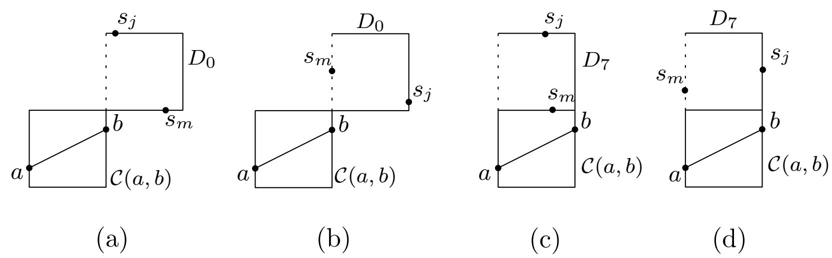

Figure 9: Cases (a) and (b) contradict Claim 4.2. Case (c) contradicts our general position assumption. In case (d) only one point, s_j, is associated to D_7.

position assumption implies that $s_m = b$, since $s_m \neq a$. Thus, $d_\Box(s_j, u_j) > 2 = d_\Box(s_j, s_m)$, which contradicts Claim 4.2. Therefore, there is only one point associated to D_i.

Finally, if D_i contains a, then there is no point s'_j in D_i. Indeed, assume for sake of a contradiction that $s'_j \in D_i$. Then, s_j is not in D_i, otherwise, $d_\Box(a, s_j) < d_\Box(s_j, u_j)$, contradicting Claim 4.1. Thus, s'_j is on $D_i \cap \partial D_\Box(\bar{o}, 3)$ and $s_j = \lambda s'_j$ for some $\lambda > 1$. Hence, $d_\Box(s'_j, a) = 2$, which means that $a \in D_\Box(s'_j, 2)$. Let p be the point $\bar{o}s'_j \cap \partial\mathcal{C}(a, b)$. By Claim 3.5, $D_\Box(s'_j, 2) \subset D_\Box(s_j, d_\Box(s_j, p))$. So, $a \in D_\Box(s_j, d_\Box(s_j, p))$ and $d_\Box(s_j, a) < d_\Box(s_j, u_j)$, contradicting Claim 4.1. $\Box$

Theorem 5.3. *For any set S of points in general position, the graph 7-$GG_\Box(S)$ is Hamiltonian.*

Proof. From Lemma 5.2 we have that for each $0 \leq i \leq 7$ there is at most one point of $\{a, s'_1, \ldots, s'_k\}$ associated to D_i, and any square containing a has no s'_i associated to it. Since there is at least one D_i containing a, there are at most 7 points s'_j in $D_\Box(\bar{o}, 3)$. Therefore, there are at most 7 points of S in the interior of $\mathcal{C}(a, b)$, and the bottleneck Hamiltonian cycle of S is contained in 7-$GG_\Box(S)$. $\Box$

5.2 Hamiltonicity for regular hexagons

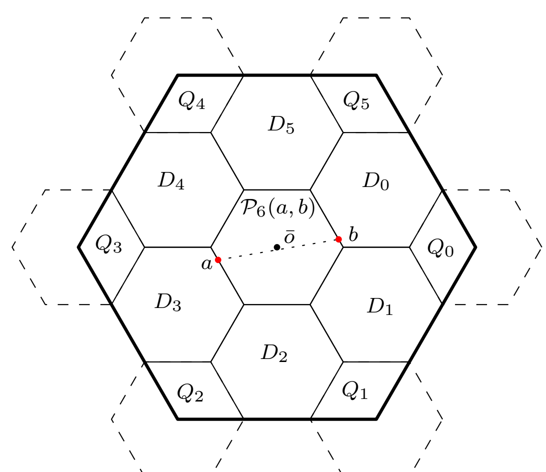

Figure 10: The bold hexagon is the boundary of $D_{\mathcal{P}_6}(\bar{o}, 3)$. Such hexagon is divided into 13 interior-disjoint regions: 6 quadrangles—a third of a unit $\mathcal{P}_6$-disk—and 7 unit $\mathcal{P}_6$-disks.

The analysis for the case of hexagons is similar to the previous one. First we divide the hexagon $D_{\mathcal{P}_6}(\bar{o}, 3)$ into 13 different regions $\mathcal{C}(a, b), D_0, \ldots, D_5, Q_0, \ldots, Q_5$, shown in Fig. 10. Let indices be taken modulo 6. We will associate a point in $D_{\mathcal{P}_6}(\bar{o}, 3)$ (not in the interior of $\mathcal{C}(a, b)$) to a region D_i or Q_i in the following fashion. If a point is in the interior of D_i or Q_i we say that such point is associated to D_i or Q_i, respectively. If a point is on the edge $D_i \cap D_{i-1}$ or edge $D_i \cap Q_{i-1}$, then such point is associated to D_{i-1} and Q_{i-1}, respectively. In the case when a point is the vertex $D_i \cap D_{i-1} \cap Q_{i-1}$, we say that such point is associated to D_{i-1}. When a point is on the edge $D_i \cap Q_i$ then we associate it with D_i. See Fig. 11.

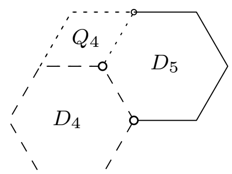

Figure 11: The dashed boundary of D_5 is associated to D_4 and the dotted one is associated to Q_4. The rest of D_5 is associated to D_5.

Observation 5.4. *Any two points at $d_{\mathcal{P}_6}$-distance 2 in a unit hexagon D must be on opposite sides of D.*

In the following lemma we show that the hexagon $D_{\mathcal{P}_6}(\bar{o}, 3)$ contains at most 11 points $s'_1, \ldots, s'_k$.

Lemma 5.5. *There is at most one point s'_j associated to each region of type D_i or Q_i. Moreover, there is no point s'_j in the hexagon D_i that contains a.*

Proof. If a point is in the interior of D_i or Q_i then by Observation 5.4 there is no other point in the same region.

Note that if Q_i contains two points at $d_{\mathcal{P}_6}$-distance 2, then by Observation 5.4 such points are exactly $D_i \cap Q_i \cap \partial D_{\mathcal{P}_6}(\bar{o}, 3)$ and $D_{i+1} \cap Q_i \cap \partial D_{\mathcal{P}_6}(\bar{o}, 3)$. Since the points on $D_i \cap Q_i$ are associated to D_i, the intersection point $D_i \cap Q_i \cap \partial D_{\mathcal{P}_6}(\bar{o}, 3)$ is not associated to Q_i. Thus, there is at most one point associated to Q_i.

If D_i contains a point s'_j that is on $D_i \cap \partial D_{\mathcal{P}_6}(\bar{o}, 3)$, then there cannot be another $s'_m \in D_i$: Otherwise, by Observation 5.4, s'_m would be on the boundary of $\mathcal{P}_6(a, b)$, in which case $s'_m = b$ due to our general position assumption. Since, $d_{\mathcal{P}_6}(s'_j, s'_m) = 2$, it follows from Lemma 4.3 that s_j would be in $D_{\mathcal{P}}(\bar{o}, 3)$. Thus, $d_{\mathcal{P}_6}(s_j, s_m) = 2 < d_{\mathcal{P}_6}(s_j, u_j)$ which contradicts Claim 4.2. Consequently, if D_i contains two points s'_j and s'_m then by Observation 5.4 either: 1) one is on the edge $D_i \cap Q_i$ and the other is on the edge $D_i \cap D_{i-1}$ (see Fig. 12a); or 2) one is on the edge $D_i \cap D_{i+1}$ and the other is on the edge $D_i \cap Q_{i-1}$ (see Fig. 12b). In either case, just one point is associated to D_i.

Finally, if D_i contains a, then there is no point s'_j in D_i. Indeed, suppose for sake of contradiction that $s'_j \in D_i$. Then, s_j is not in D_i because, by Claim 4.1, $d_{\mathcal{P}_6}(a, s_j) \geq d_{\mathcal{P}_6}(s_j, u_j)$. Thus, s'_j is on $D_i \cap \partial D_{\mathcal{P}_6}(\bar{o}, 3)$ and $s_j = \lambda s'_j$ for some $\lambda > 1$. Hence, $d_{\mathcal{P}_6}(s'_j, a) = 2$ and $a \in D_{\mathcal{P}_6}(s'_j, 2)$. Let p be the intersection point $\bar{o}s'_j \cap \partial \mathcal{P}_6(a, b)$. By Claim 3.5, $D_{\mathcal{P}_6}(s'_j, 2) \subset D_{\mathcal{P}_6}(s_j, d_{\mathcal{P}_6}(s_j, p))$ and, thus, $a \in D_{\mathcal{P}_6}(s_j, d_{\mathcal{P}_6}(s_j, p))$. We obtain that $d_{\mathcal{P}_6}(s_j, a) < d_{\mathcal{P}_6}(s_j, u_j)$, which again contradicts Claim 4.1. □

The following theorem holds.

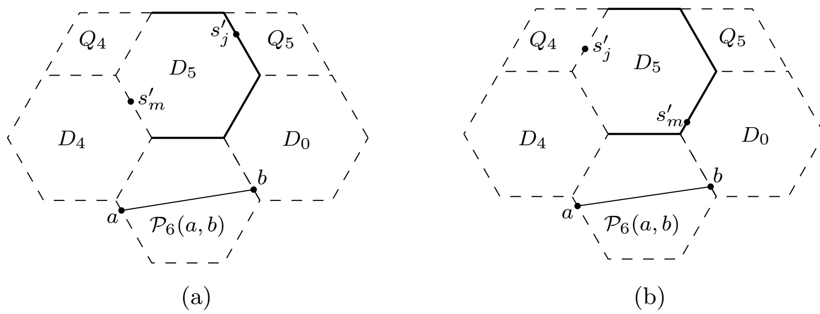

Figure 12: In both, (a) and (b), D_5 contains exactly two points at $d_{\mathcal{P}_6}$-distance 2.

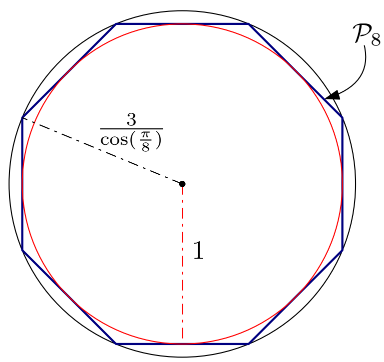

Figure 13: The incircle of the octagon $\mathcal{P}_8$ has Euclidean radius 1. The octagon $\mathcal{P}_8$ is inscribed in a circle of Euclidean radius $\frac{3}{\cos(\frac{\pi}{8})}$; such circle is also known as the circumcircle of $\mathcal{P}_8$.

Theorem 5.6. *For any set S of points in general position, the graph 11-$GG_{\mathcal{P}_6}(S)$ is Hamiltonian.*

5.3 Hamiltonicity for regular even-sided t-gons where $t \geq 8$

For the remaining regular polygons with an even number of sides, we use the circumcircle [8] of $D_{\mathcal{P}_t}(\bar{o}, 3)$ in order to give an upper bound on the number of points in $D_{\mathcal{P}_t}(\bar{o}, 3)$ at pairwise Euclidean distance at least 2. Without loss of generality we assume that the incircle [9] of the unit $\mathcal{P}_t$-disk has Euclidean radius 1. See Fig. 13.

In this section we will first treat the case $t \geq 10$, and afterwards the case $t = 8$.

Theorem 5.7. *For any set S of points in general position and regular polygon $\mathcal{P}_t$ with even $t \geq 10$, the graph 11-$GG_{\mathcal{P}_t}(S)$ is Hamiltonian.*

Proof. Let $\mathcal{P}_t$ be a polygon with $t \geq 10$ sides and t even. Then $D_{\mathcal{P}_t}(\bar{o}, 3)$ is inscribed in a circle of radius $r = \frac{3}{\cos(\frac{\pi}{t})}$. Since the function $\cos(\frac{\pi}{t})$ is an increasing function for $t \geq 2$, we have that $r \leq \frac{3}{\cos(\frac{\pi}{10})}$. Therefore, $D_{\mathcal{P}_t}(\bar{o}, 3)$ is inside the circumcircle of a decagon with incircle of radius 3. In addition, from Lemma 4.3 we know that for any pair of points s'_i, s'_j in $D_{\mathcal{P}_t}(\bar{o}, 3)$, $d_{\mathcal{P}_t}(s'_i, s'_j) \geq 2$. Since the incircle of the 2-unit $\mathcal{P}_t$-disk has Euclidean radius 2, we

[8]The *circumcircle* of a polygon $\mathcal{P}$ is the smallest circle that contains $\mathcal{P}$.

[9]The *incircle* of a polygon $\mathcal{P}$ is the largest circle in the interior of $\mathcal{P}$ that is tangent to each side of $\mathcal{P}$.

have that $d(s'_i, s'_j) \geq 2$. Hence, it suffices to show that there are at most 12 points in $D_{\mathcal{P}_t}(\bar{o}, 3)$ at pairwise Euclidean distance at least 2. Fodor [13] proved that the minimum radius R of a circle having 13 points at pairwise Euclidean distance at least 2 is $R \approx 3.236$, which is greater than $\frac{3}{\cos(\frac{\pi}{10})} \approx 3.154$. Thus, $D_{\mathcal{P}_t}(\bar{o}, 3)$ contains at most 12 points at pairwise $d_{\mathcal{P}_t}$-distance at least 2. Since a is also at $d_{\mathcal{P}_t}$-distance at least 2 from all s'_i's, there are at most 11 points of S inside $\mathcal{P}_t(a, b)$. □

For the case of octagons, the radius of the circumcircle of $D_{\mathcal{P}_8}(\bar{o}, 3)$ is greater than 3.236, so we cannot use the result in [13]. However, we can use a similar result from Fodor [14] to prove an analogous theorem:

Theorem 5.8. *For any set S of points in general position, the graph 12-$GG_{\mathcal{P}_8}(S)$ is Hamiltonian.*

Proof. From Lemma 4.3 we know that, for any pair of points s'_i, s'_j in $D_{\mathcal{P}_8}(\bar{o}, 3)$, $d_{\mathcal{P}_8}(s'_i, s'_j) \geq 2$. Since the incircle of the 2-unit $\mathcal{P}_8$-disk has Euclidean radius 2, we have that $d(s'_i, s'_j) \geq 2$. Hence, it suffices to show that there are at most 13 points in $D_{\mathcal{P}_8}(\bar{o}, 3)$ at pairwise Euclidean distance at least 2. The regular octagon $D_{\mathcal{P}_8}(\bar{o}, 3)$ is inscribed in a circle of radius $r = \frac{3}{\cos(\frac{\pi}{8})} \approx 3.247$. By a result of Fodor [14], the smallest radius R of a circle containing 14 points at pairwise Euclidean distance at least 2 is $R \approx 3.328$. Hence, $D_{\mathcal{P}_8}(\bar{o}, 3)$ contains at most 13 points at pairwise Euclidean distance at least 2. Since a is also at $d_{\mathcal{P}_8}$-distance at least 2 from all s'_i's, there are at most 12 points of S inside $\mathcal{P}_8(a, b)$. □

6 Lower bounds for the existence of bottleneck Hamiltonian cycles in k-$GG_\square$ and k-$GG_{\mathcal{P}_6}$

In this section we give lower bounds on the minimum values of k for which the graphs k-$GG_\square$ and k-$GG_{\mathcal{P}_6}$ contain a bottleneck Hamiltonian cycle. This is useful to understand to what extent we can use the bottleneck Hamiltonian cycle for showing Hamiltonicity in a k-$GG_{\mathcal{C}}$ in order to improve the known upper bounds on k. The proofs are very similar to those in [5, 6, 15].

Lemma 6.1. *There exists a point set S with $n \geq 17$ points such that 2-$GG_\square(S)$ does not contain any $d_\square$-bottleneck Hamiltonian cycle of S.*

Proof. Consider the point set S in Fig. 14. The length of edge ab is $d_\square(a, b) = 1$, and the two dashed squares have radius 1 and are centered at a and b. Notice that any $\mathcal{C}(a, b)$ contains at least 3 points from $U = \{u_1, u_2, u_3, u_4\}$, so $ab \notin$ 2-$GG_\square(S)$.

Let $R = \{r_1, r_2, r_3, r_4, t_1, \ldots t_7\}$. For each point in R there is a red square centered at such point with radius $1+\varepsilon$, where ε is a small positive value. Thus, $d_\square(r_i, u_i) = 1+\varepsilon$, $d_\square(r_i, a) > 1+\varepsilon$, $d_\square(r_i, b) > 1+\varepsilon$ and $d_\square(r_i, r_j) > 1+\varepsilon$, for $i \neq j$. The cycle h=$(a, b, u_1, r_1, u_2, r_2, t_1, t_2, t_3, t_4, t_5, t_6, t_7, r_3, u_3, r_4, u_4, a)$ is Hamiltonian and the maximum length of its edges in the $d_\square$-distance is $1+\varepsilon$. Hence, any $d_\square$-bottleneck Hamiltonian cycle of S has at most $1+\varepsilon$ maximum edge $d_\square$-length.

We will show that the edge ab is in every $d_\square$-bottleneck Hamiltonian cycle of S. Let h' be a $d_\square$-bottleneck Hamiltonian cycle. Since the $d_\square$-distance from a and b to any point in R is greater than $1+\varepsilon$, in h', a and b can only be connected between each other or to the points in U. Note that u_2 has to be connected to r_1 and r_2 in h', since otherwise r_1 or r_2 would be

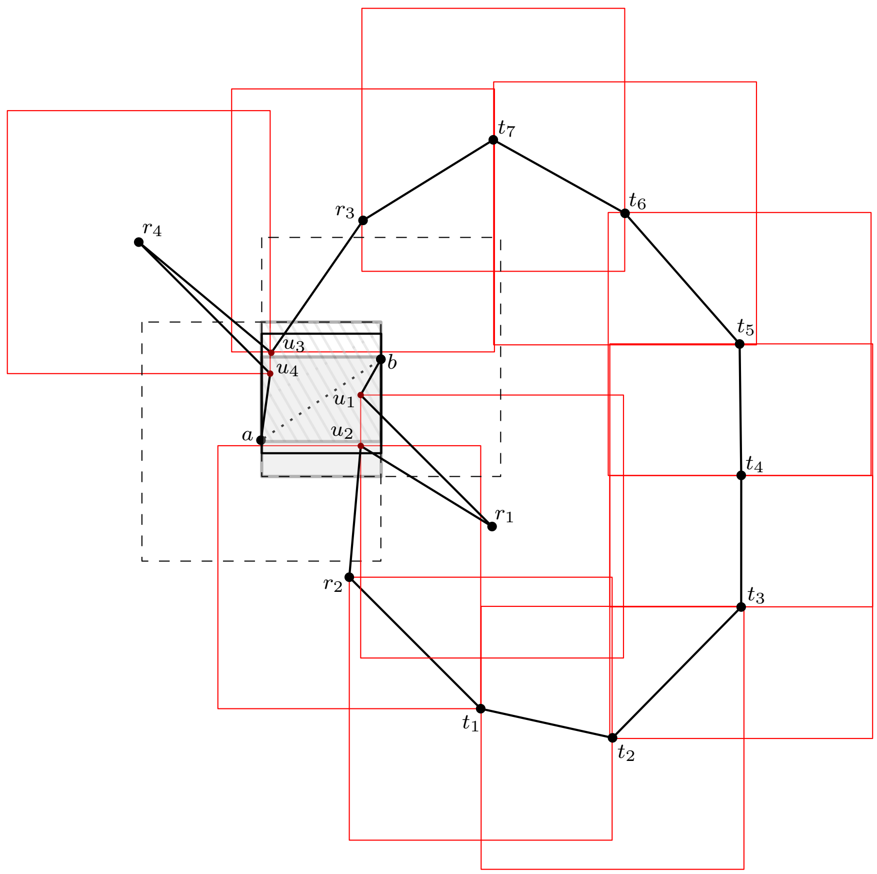

Figure 14: The diagonal-pattern square is a $\mathcal{C}(a,b)$ with a as a vertex, and the gray-filled square is a $\mathcal{C}(a,b)$ with b as vertex. The union of both squares contains all the possible $\mathcal{C}(a,b)$. The bold edges belong to h in the proof of Lemma 6.1.

adjacent to an edge whose $d_\square$-length is greater than $1+\varepsilon$. Similarly, u_3 has to be connected to r_3 and r_4 in h', since otherwise r_3 or r_4 would be adjacent to an edge of $d_\square$-length greater than $1+\varepsilon$. Finally, a and b have to be connected to each other, since otherwise both would be adjacent to u_1 and u_4, which does not produce a Hamiltonian cycle.

In summary, ab is included in any $d_\square$-bottleneck Hamiltonian cycle, and since $ab \notin$ 2-$GG_\square(S)$, the lemma holds. □

Lemma 6.2. *There exists a point set S with $n \geq 22$ points such that 5-$GG_{\mathcal{P}_6}(S)$ does not contain any $d_{\mathcal{P}_6}$-bottleneck Hamiltonian cycle of S.*

Proof. We proceed in the same fashion as in the previous proof. Consider the point set S in Fig. 15. The length of edge ab is $d_{\mathcal{P}_6}(a,b)=1$, and the dashed hexagons have radius 1 and are centered at a and b. Notice that there is exactly one $\mathcal{C}(a,b)$, and it contains all points from $U=\{u_1,\dots,u_6\}$. Therefore, $ab \notin$ 5-$GG_{\mathcal{P}_6}(S)$. Let $R=\{r_1,\dots,r_6,t_1,\dots t_8\}$. For each point in R there is a red regular hexagon centered at such point with radius $1+\varepsilon$, where ε is a small positive value. Thus, $d_{\mathcal{P}_6}(r_i,u_i)=1+\varepsilon$, $d_{\mathcal{P}_6}(r_i,a)>1+\varepsilon$, $d_{\mathcal{P}_6}(r_i,b)>1+\varepsilon$ and $d_{\mathcal{P}_6}(r_i,r_j)>1+\varepsilon$, with $i\neq j$. The cycle $h=(a,b,u_1,r_1,\ u_2,r_2,u_3,r_3,t_1,t_2,\dots,\ t_8,r_4,u_4,r_5,u_5,r_6,u_6,a)$ is Hamiltonian, and the maximum length of its edges in the $d_{\mathcal{P}_6}$-distance is $1+\varepsilon$.

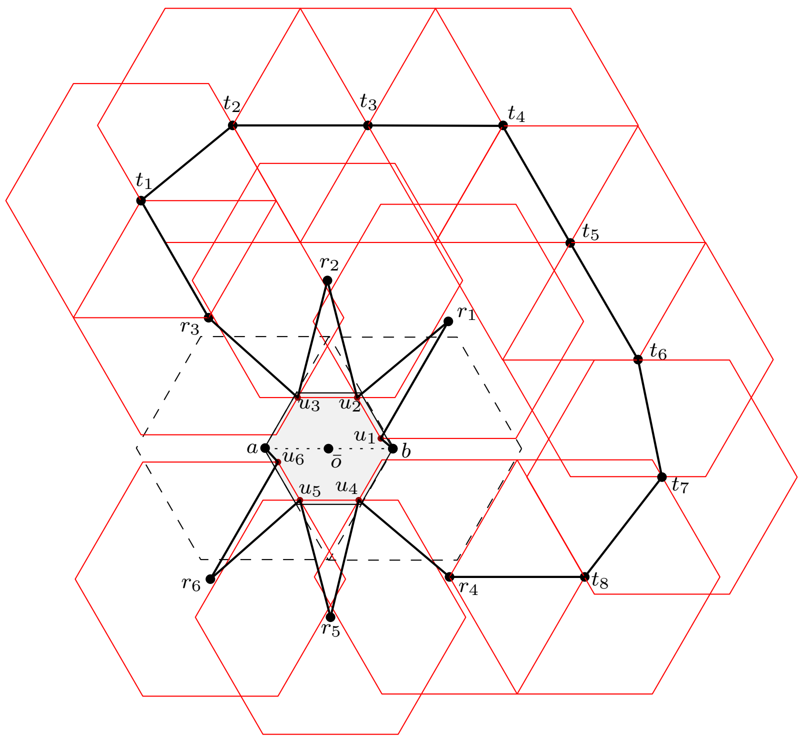

Figure 15: The gray hexagon is the unique $\mathcal{C}(a, b)$, and it contains 6 points of S. The bold edges belong to h in the proof of Lemma 6.2.

Let h' be a $d_{\mathcal{P}_6}$-bottleneck Hamiltonian cycle. Let us show that $ab \in h'$. Since the $d_{\mathcal{P}_6}$-distance from a and b to any point in R is greater than $1 + \varepsilon$, in h', a and b can only be connected between each other or to the points in U. Note that u_3 has to be adjacent to r_2 and r_3; otherwise, r_2 or r_3 would be adjacent to an edge of $d_{\mathcal{P}_6}$-length greater than $1 + \varepsilon$. Similarly, u_2, u_4, u_5 have to be adjacent to r_2 and r_3, to r_4 and r_5, and to r_5 and r_6, respectively. Finally, a and b have to be connected to each other, otherwise both would be adjacent to u_1 and u_6 which does not produce a Hamiltonian cycle. Therefore, ab is included in any $d_{\square}$-bottleneck Hamiltonian cycle, and since $ab \notin 5\text{-}GG_{\mathcal{P}_6}(S)$, the lemma holds. □

7 Non-Hamiltonicity for regular polygons

Until now we have discussed upper and lower bounds for k, so that $k\text{-}GG_{\mathcal{C}}$ contains a bottleneck Hamiltonian cycle. As mentioned in Section 2, $k\text{-}GG_{\mathcal{C}} \subseteq k\text{-}DG_{\mathcal{C}}$, thus all upper bounds given in the previous sections hold for k-order $\mathcal{C}$-Delaunay graphs as well, but not the lower bounds. In this section we present point sets for which $DG_{\mathcal{P}_t}$ is not Hamiltonian. For $t = 4$, Saumell [18] showed that for any $n \geq 9$ there exists a point set S such that $DG_{\square}(S)$ is non-Hamiltonian, so we focus on $t \geq 5$.

First, we present particular cases of $t \geq 5$ for which $DG_{\mathcal{P}_t}$ is non-Hamiltonian. Later on, we present a generalization of these point sets and show the non-Hamiltonicity for an infinite family of $DG_{\mathcal{P}_t}$.

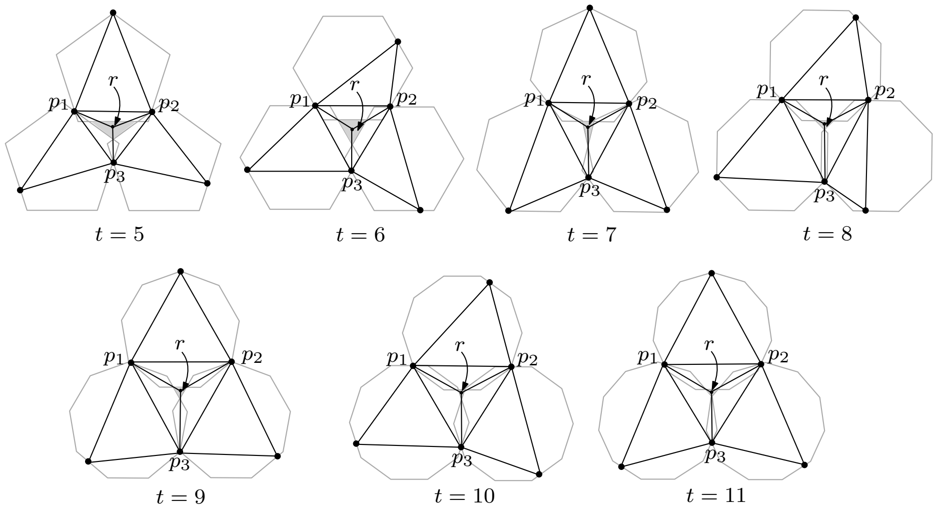

Figure 16: For each $t \in \{5, 6, 7, 8, 9, 10, 11\}$ the graph $DG_{\mathcal{P}_t}(S)$ is non-Hamiltonian.

7.1 Non-Hamiltonicity for regular polygons with small number of sides

In this section we prove that $DG_{\mathcal{P}_t}$ fails to be Hamiltonian for every point set when $t = 5, 6, \ldots, 11$ (see Fig. 16).

Lemma 7.1. *For any $n \geq 7$ and any $t \in \{5, 6, \ldots, 11\}$, there exists an n-point set S such that $DG_{\mathcal{P}_t}(S)$ is non-Hamiltonian.*

Proof. Let $t \in \{5, 6, \ldots, 11\}$. Consider the graph $DG_{\mathcal{P}_t}(S)$ in Fig. 16 for such t. Note that such graph is indeed a $\mathcal{P}_t$-Delaunay graph, since for each edge there exists a $\mathcal{P}_t$-disk that contains its vertices on its boundary and is empty of other points of S. Also, note that some edges from the convex hull of S do not appear in such graphs. Finally, notice that there exists an area r that is not contained in any of the $\mathcal{P}_t$-disks associated to the edges of the outer face or the triangle $\triangle p_1p_2p_3$. Such area can have an arbitrary number of points in its interior, say $n-6$. Now, let $G' = DG_{\mathcal{P}_t}(S) \setminus \{p_1, p_2, p_3\}$. The graph G' consists of 4 connected components, so $DG_{\mathcal{P}_t}(S)$ is not 1-tough. Since every Hamiltonian graph is 1-tough, $DG_{\mathcal{P}_t}(S)$ is non-Hamiltonian. □

7.2 An infinite family of regular polygons such that $DG_{\mathcal{P}_t}$ is non-Hamiltonian

Based on the point sets given in the previous section, we construct an n-point set S, with $n \geq 7$, such that the following theorem holds.

Theorem 7.2. *Let $\mathcal{P}_t$ be a regular t-gon, where $t > 3$ and t is an odd number and multiple of three. For any $n \geq 7$, there exists an n-point set S such that $DG_{\mathcal{P}_t}(S)$ is non-Hamiltonian.*

Our construction is a generalization of the ones in the previous section. However, in order to be able to prove that $DG_{\mathcal{P}_t}(S)$ has the desired structure for arbitrary large values of t, we have to define it in a very precise way.

Before we proceed to prove Theorem 7.2, we need some new definitions and a few auxiliary claims.

Let $\mathcal{P}_t$ be a regular t-gon, where $t = 3(2m+1)$ for some positive integer m. Without loss of generality, we assume that $\mathcal{P}_t$ is oriented so that its bottom side is horizontal. We also assume that its vertices are given in counterclockwise order.

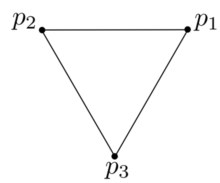

Figure 17: An equilateral triangle pointing downwards.

Consider three points p_1, p_2 and p_3 in the plane that define an equilateral triangle T as in Fig. 17. Let c be the circumcenter of the triangle T. Let C_1, C_2 and C_3 be three circles circumscribing the triangles $\triangle p_1p_2c$, $\triangle p_2p_3c$ and $\triangle p_3p_1c$, respectively. These three circles are *Johnson circles*,[10] they have the same radius r, and they intersect at c. Let c_1, c_2 and c_3 be the centers of C_1, C_2 and C_3, respectively. Notice that the line segments p_2c_2 and c_3p_1 are vertical, and that $\angle cc_ip_{i+1} = \frac{\pi}{3}$ and $\angle p_ic_ic = \frac{\pi}{3}$, for all i modulo 3. See Fig. 18.

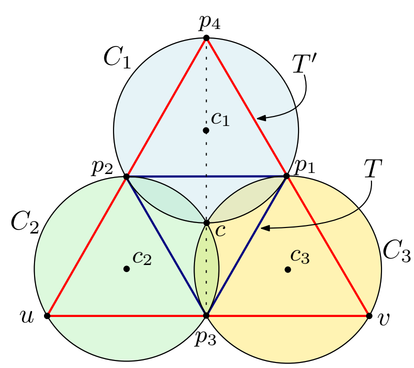

Figure 18: The circles C_1, C_2, C_3 contain triangles $\triangle p_1p_2c$, $\triangle p_2p_3c$ and $\triangle p_3p_1c$, respectively. The big triangle $T' = \triangle p_4uv$ is the anticomplementary triangle of T.

Consider the *anticomplementary triangle*[11] $T' = \triangle p_4uv$ of T defined as in Fig. 18. Let $\mathcal{P}_t^1, \mathcal{P}_t^2$ and $\mathcal{P}_t^3$ be the three t-gons inscribed in C_1, C_2 and C_3, respectively. See Fig. 19.

[10] A set of *Johnson circles* is a set of three circles of the same size that mutually intersect each other in a single point. For a survey about the properties of Johnson circles, we refer the reader to the *Johnson Theorem* [16].

[11] Let C be the circle with center $C_1 \cap C_2 \cap C_3$ and radius $2r$. The *anticomplementary triangle* of T has as vertices the three tangent points of C with the Johnson circles.

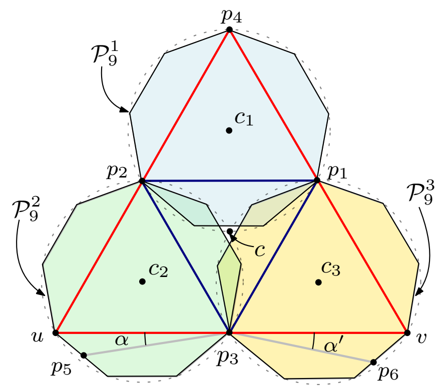

Figure 19: Inscribed t-gons for $t = 9$. The angles α and α' are less than $\frac{\pi}{9}$.

Claim 7.3. *The points p_1, p_2 and p_3 are on $\partial\mathcal{P}_t^3 \cap \partial\mathcal{P}_t^1$, $\partial\mathcal{P}_t^1 \cap \partial\mathcal{P}_t^2$ and $\partial\mathcal{P}_t^2 \cap \partial\mathcal{P}_t^3$, respectively.*

Proof. Recall that $t = 3(2m+1)$ with $m > 0$. Let a_1b_1 be the bottom side of $\partial\mathcal{P}_t^1$. Since the line segment c_1c is vertical, c_1c bisects a_1b_1. Thus, the angle formed by c_1c and the i-th vertex of $\partial\mathcal{P}_t^1$ is given by $\frac{\pi}{t} + \frac{2(i-1)\pi}{t}$. In particular, for $i = m+1$ we obtain $\frac{2m\pi}{t} + \frac{\pi}{t} = \frac{(2m+1)\pi}{3(2m+1)} = \frac{\pi}{3}$, which is precisely $\angle cc_1p_2$. Hence, $p_2 \in \partial\mathcal{P}_t^1$. The proof for $p_1 \in \partial\mathcal{P}_t^1$ is symmetric.

Since the bottom sides of $\partial\mathcal{P}_t^2$ and $\partial\mathcal{P}_t^3$ are horizontal, the top-most vertices of $\partial\mathcal{P}_t^2$ and $\partial\mathcal{P}_t^3$ are p_2 and p_1, respectively. Therefore $p_1 \in \partial\mathcal{P}_t^1 \cap \partial\mathcal{P}_t^3$ and $p_2 \in \partial\mathcal{P}_t^1 \cap \partial\mathcal{P}_t^2$.

On the other hand, since the top-most point of $\partial\mathcal{P}_t^2$ is p_2, the angle formed by p_2c_2 and the i-th vertex of $\partial\mathcal{P}_t^2$ is given by $\frac{2i\pi}{t}$. In particular, for $i = 2m+1$ we obtain $\frac{2(2m+1)\pi}{3(2m+1)} = \frac{2\pi}{3}$, which is precisely $\angle p_2c_2p_3$. Thus, $p_3 \in \partial\mathcal{P}_t^2$. Similarly, we can show $p_3 \in \partial\mathcal{P}_t^3$. $\square$

Given points a and b, we next show how to define a polygon which we call the *$\mathcal{P}_t$-of-influence of a and b*. Recall that the vertices $v_1, \ldots, v_t$ of $\mathcal{P}_t$ are oriented counterclockwise, where v_1 is the top-most one. The i-th oriented edge of $\mathcal{P}_t$ is defined by $e_i = \overrightarrow{v_iv_{i+1}}$. We define the oriented line ℓ_i as the supporting line of the edge e_i with the same orientation as e_i. For each ℓ_i, we consider two oriented lines parallel to ℓ_i, one passing through a and another through b. Among all these lines, we only take those having a and b on its left or on the line. Now, consider the left half-planes defined by such oriented lines; the intersection of these half-planes defines the $\mathcal{P}_t$-of-influence of a and b. See Fig. 20a. Since a point p is in a $\mathcal{P}_t$-disk if p is on the left of each supporting line ℓ_i or on ℓ_i, any $\mathcal{P}_t$-disk containing a and b contains their $\mathcal{P}_t$-of-influence.

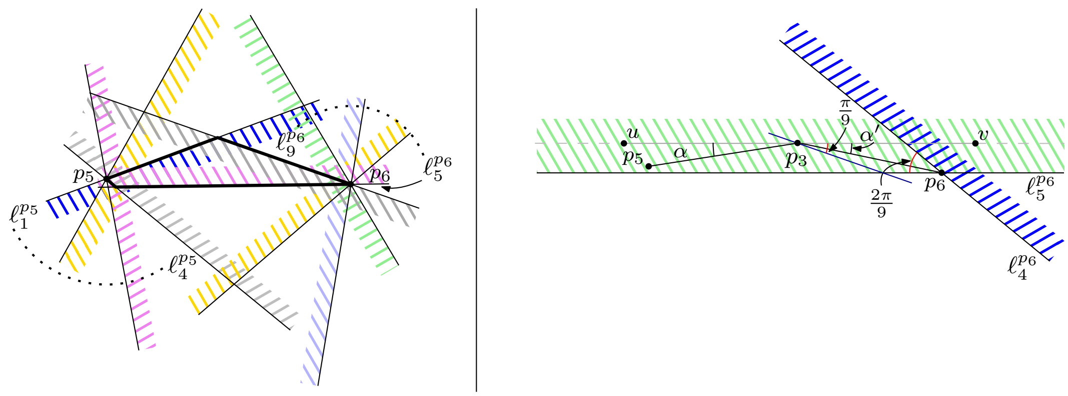

(a) (b)

Figure 20: The dashed area next to each line represents the half-plane with points on the left of the line. (a) The bold polygon is the $\mathcal{P}_9$-of-influence of p_5 and p_6. (b) The points p_5 and p_3 are on the left of $\ell_5^{p_6}$ and on the right of $\ell_4^{p_6}$.

Let p_5 and p_6 be two points on the boundary of $\mathcal{P}_t^2$ and $\mathcal{P}_t^3$, respectively, such that $\alpha = \angle p_5 p_3 u < \frac{\pi}{t}$ and $\alpha' = \angle v p_3 p_6 < \frac{\pi}{t}$. See Fig. 19.

Claim 7.4. *Any $\mathcal{P}_t$-disk containing p_5 and p_6 on its boundary contains p_3 in its interior.*

Proof. Note that if p_3 is in the interior of the $\mathcal{P}_t$-of-influence of p_6 and p_5 then the claim follows. Let us show first that p_3 is in the $\mathcal{P}_t$-of-influence of p_6 and p_5 (but not necessarily in its interior). We denote by ℓ_i^p the parallel line to ℓ_i passing through point p. Without loss of generality assume that p_5 is above the horizontal line passing through p_6. Note that α' is equal to the inner angle at p_6 formed by the horizontal line passing through p_6 and edge p_6p_3, and this angle is less than $\frac{\pi}{t}$. Also, note that for $h = \frac{t-1}{2} + 1$, ℓ_h is horizontal. Finally, observe that the angle formed by consecutive ℓ_i^p and ℓ_{i+1}^p is $\frac{2\pi}{t}$. Then, p_3 is contained in the wedge defined by $\ell_h^{p_6}$ and $\ell_{h-1}^{p_6}$ with inner angle $\frac{2\pi}{t}$ that lies above $\ell_h^{p_6}$. Refer to Fig. 20b. Since $\alpha' < \frac{\pi}{t}$, this wedge contains the wedge defined by edge p_6p_3 and $\ell_h^{p_6}$, which contains p_5. Thus, p_5 is on the left of $\ell_h^{p_6}$ and on the right of $\ell_{h-1}^{p_6}$. The lines of the form $\ell_i^{p_6}$ that have p_5 on its left are the ones encountered when rotating $\ell_h^{p_6}$ along p_6 counterclockwise until it hits p_5; the total angle of rotation is π minus the inner angle formed by p_5p_6 and $\ell_h^{p_6}$. Therefore, these lines are $\ell_h^{p_6}, \ell_{h+1}^{p_6}, \ldots, \ell_t^{p_6}$. Since the wedge defined by $\ell_h^{p_6}$ and $\ell_t^{p_6}$ containing p_5 has angle $\frac{\pi}{t}$, p_3 also lies on such wedge and p_3 is on the left of $\ell_t^{p_6}$. Moreover, the angle of the cone containing p_5 formed by $\ell_h^{p_6}$ and $\ell_i^{p_6}$, for any $i \in \{h+1, \ldots, t\}$, is at least $\frac{\pi}{t}$. Hence, p_3 lies on the left of $\ell_i^{p_6}$ for all $i \in \{h, \ldots, t\}$. Similarly, we show that $\ell_i^{p_5}$ has p_6 on its left if and only if $i = \{1, \ldots, \frac{t-1}{2}\}$, and these lines also have p_3 on its left. Thus, p_3 is in the $\mathcal{P}_t$-of-influence of p_5 and p_6. Moreover, since p_3 is strictly on the left of all the mentioned relevant lines, p_3 is in the interior of the $\mathcal{P}_t$-of-influence of p_5 and p_6. Therefore, p_3 is in the interior of any $\mathcal{P}_t$-disk containing p_5 and p_6. □

Now, we proceed to prove Theorem 7.2.

Proof of Theorem 7.2. Since the bottom side e_b of $\mathcal{P}_t^1$ is horizontal and the intersection of the three circles C_1, C_2, C_3 is only the point c, there is an empty space in C_1 bounded by e_b

and the circular arcs of C_2 and C_3 with endpoints c and the intersection points $e_b \cap C_2$ and $e_b \cap C_3$. Let us call such area A_c. See Fig. 21. Let S' be a set of $n-6$ points in general position contained in A_c. Let $S = \{p_1, p_2, p_3, p_4, p_5, p_6\} \cup S'$.

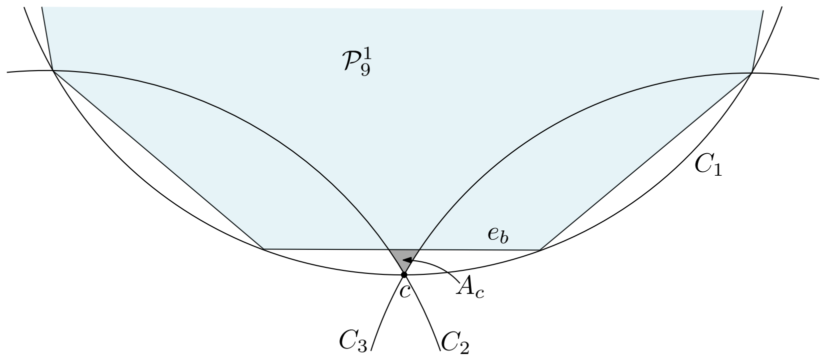

Figure 21: The gray area A_c is contained in the interior of $C_1 \setminus (C_2 \cup C_3)$ and is not contained in $\mathcal{P}_9^1$.

Since for $i = 1, 2, 3$ the $\mathcal{P}_t$-disk $\mathcal{P}_t^i$ contains no point of S in its interior, from Claim 7.3 it follows that the edges p_1p_2, p_2p_3, p_3p_1 are in $DG_{\mathcal{P}_t}(S)$.[12] Also, since for each of the edges p_5p_2, p_2p_4, p_4p_1, p_1p_6, p_6p_3 and p_3p_5, its endpoints lie on $\partial\mathcal{P}_t^i$ for some fixed $i \in \{1, 2, 3\}$, such edges are in $DG_{\mathcal{P}_t}(S)$. By Claim 7.4, $p_5p_6 \notin DG_{\mathcal{P}_t}(S)$. Hence, the outerface of $DG_{\mathcal{P}_t}(S)$ is given by the edges $p_5p_2, p_2p_4, p_4p_1, p_1p_6, p_6p_3$ and p_3p_5.

The graph $DG_{\mathcal{P}_t}(S)$ is not 1-tough because $DG_{\mathcal{P}_t}(S) \setminus \{p_1, p_2, p_3\}$ consists of four connected components, namely, $\{p_4\}, \{p_5\}, \{p_6\}$ and $DG_{\mathcal{P}_t}(S')$. Therefore, $DG_{\mathcal{P}_t}(S)$ is not Hamiltonian. □

8 Conclusions

In this paper we have presented the first general results on Hamiltonicity for higher-order convex-shape Delaunay and Gabriel graphs. By combining properties of metrics and packings, we have achieved general bounds for any convex shape, and improved bounds for point-symmetric shapes, as well as for even-sided regular polygons. For future research, we point out that our results are based on bottleneck Hamiltonian cycles, in the same way as all previously obtained bounds [1, 9, 15]. However, in several cases, as we show in Section 6, this technique is reaching its limit. Therefore a major challenge to effectively close the existing gaps will be to devise a different approach to prove Hamiltonicity of Delaunay graphs.

References

[1] Manuel Abellanas, Prosenjit Bose, Jesús García-López, Ferran Hurtado, Carlos M. Nicolás, and Pedro Ramos. On structural and graph theoretic properties of higher order Delaunay graphs. *Internat. J. Comput. Geom. Appl.*, 19(6):595–615, 2009.

[12] Notice that each of the $\mathcal{P}_t^i$ satisfies the following property: For any two of the three points of S on its boundary, the $\mathcal{P}_t$-disk can be slightly perturbed so that the two chosen points remain on its boundary and the third point lies in the exterior of the $\mathcal{P}_t$-disk.

[2] Bernardo M Ábrego, Esther M Arkin, Silvia Fernández-Merchant, Ferran Hurtado, Mikio Kano, Joseph SB Mitchell, and Jorge Urrutia. Matching points with squares. *Discrete Comput. Geom.*, 41(1):77–95, 2009.

[3] Franz Aurenhammer, Rolf Klein, and Der-Tsai Lee. *Voronoi diagrams and Delaunay triangulations*. World Scientific Publishing Company, 2013.

[4] Franz Aurenhammer and Günter Paulini. On shape Delaunay tessellations. *Inf. Process. Lett.*, 114(10):535–541, 2014.

[5] Ahmad Biniaz, Anil Maheshwari, and Michiel Smid. Bottleneck matchings and Hamiltonian cycles in higher-order Gabriel graphs. In *Proceedings of the 32nd European Workshop on Computational Geometry (EuroCG16)*, pages 179–182.

[6] Ahmad Biniaz, Anil Maheshwari, and Michiel Smid. Higher-order triangular-distance Delaunay graphs: Graph-theoretical properties. *Comput. Geom.*, 48(9):646–660, 2015.

[7] Nicolas Bonichon, Cyril Gavoille, Nicolas Hanusse, and David Ilcinkas. Connections between theta-graphs, Delaunay triangulations, and orthogonal surfaces. In *International Workshop on Graph-Theoretic Concepts in Computer Science*, pages 266–278. Springer, 2010.

[8] Prosenjit Bose, Paz Carmi, Sebastien Collette, and Michiel Smid. On the stretch factor of convex Delaunay graphs. *J. Comput. Geom.*, 1(1):41–56, 2010.

[9] Maw-Shang Chang, Chuan Yi Tang, and Richard C. T. Lee. 20-relative neighborhood graphs are Hamiltonian. *J. Graph Theory*, 15(5):543–557, 1991.

[10] L. Paul Chew. There are planar graphs almost as good as the complete graph. *J. Comput. System Sci.*, 39(2):205–219, 1989.

[11] Michael B. Dillencourt. A non-Hamiltonian, nondegenerate Delaunay triangulation. *Inf. Process. Lett.*, 25(3):149–151, 1987.

[12] Michael B. Dillencourt. Toughness and Delaunay triangulations. *Discrete Comput. Geom.*, 5:575–601, 1990.

[13] Ferenc Fodor. The densest packing of 13 congruent circles in a circle. *Beitr. Algebra Geom.*, 44(2):431–440, 2003.

[14] Ferenc Fodor. Packing of 14 congruent circles in a circle. *Stud. Univ. Zilina Math. Ser*, 16:25–34, 2003.

[15] Tomáš Kaiser, Maria Saumell, and Nico Van Cleemput. 10-Gabriel graphs are Hamiltonian. *Inf. Process. Lett.*, 115(11):877–881, 2015.

[16] Dana N Mackenzie. Triquetras and porisms. *College Math. J.*, 23(2):118–131, 1992.

[17] Atsuyuki Okabe, Barry Boots, Kokichi Sugihara, and Sung Nok Chiu. *Spatial Tessellations: Concepts and Applications of Voronoi Diagrams*. Wiley, 2000.

[18] Maria Saumell Mendiola. *Some problems on proximity graphs*. PhD thesis, Universitat Politècnica de Catalunya, 2011.

[19] Michael Shamos. *Computational Geometry*. PhD thesis, Yale University, 1978.

[20] Ge Xia. The stretch factor of the Delaunay triangulation is less than 1.998. *SIAM J. Comput.*, 42(4):1620–1659, 2013.